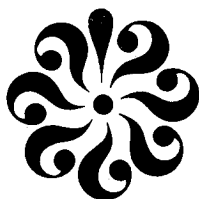


19830004806

OLD DOMINION UNIVERSITY RESEARCH FOUNDATION



DEPARTMENT OF MECHANICAL ENGINEERING AND MECHANICS  
SCHOOL OF ENGINEERING  
OLD DOMINION UNIVERSITY  
NORFOLK, VIRGINIA

OCT 82

STUDY OF HIGHLY SWEEPBACK WINGS BY THE FREE  
VORTEX SHEET METHOD

By

C. Subba Reddy, Principal Investigator

and

Farhad Ghaffari

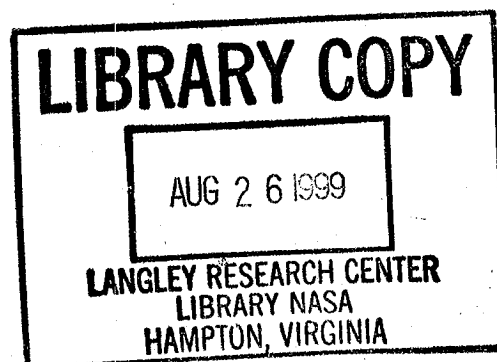
FOR REFERENCE

NOT TO BE TAKEN FROM THIS ROOM

Technical Report  
For the period ending August 15, 1982

Prepared for the  
National Aeronautics and Space Administration  
Langley Research Center  
Hampton, Virginia

Under  
Research Grant NSG 1561  
James M. Luckring, Technical Monitor  
Subsonic-Transonic Aerodynamics Division



October 1982



3 1176 01432 9057

DEPARTMENT OF MECHANICAL ENGINEERING AND MECHANICS  
SCHOOL OF ENGINEERING  
OLD DOMINION UNIVERSITY  
NORFOLK, VIRGINIA

STUDY OF HIGHLY SWEEPBACK WINGS BY THE FREE  
VORTEX SHEET METHOD

By

C. Subba Reddy, Principal Investigator

and

Farhad Ghaffari

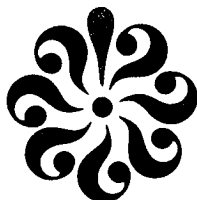
Technical Report

For the period ending August 15, 1982

Prepared for the  
National Aeronautics and Space Administration  
Langley Research Center  
Hampton, Virginia 23665

Under  
Research Grant NSG 1561  
James M. Luckring, Technical Monitor  
Subsonic-Transonic Aerodynamics Division

Submitted by the  
Old Dominion University Research Foundation  
P.O. Box 6369  
Norfolk, Virginia 23508-0369



October 1982

N83-13076

## TABLE OF CONTENTS

	<u>Page</u>
ABSTRACT.....	1
INTRODUCTION.....	1
NOMENCLATURE.....	2
RESULTS AND DISCUSSION.....	2
CONCLUSIONS.....	5
REFERENCES.....	6

## LIST OF TABLES

### Table

1	Wing configurations modeled by the FVS method.....	8
2	Comparison of aerodynamic characteristics of DM-1 glider at $\alpha = 15^\circ$ and $M = 0$ .....	11

## LIST OF FIGURES


### Figure

1	Geometry and principal dimensions of delta and double delta wing models.....	12
2	Aerodynamic characteristics of $A = 2.0$ flat delta wing- body combination at $M = 0.5$ .....	13
3	Aerodynamic characteristics of $A = 2.0$ flat delta wing- body combination at $M = 0.7$ .....	14
4	Aerodynamic characteristics of $A = 2.0$ flat delta wing- body combination at $M = 0.9$ .....	15
5	Effect of different types of modeling on spanwise pressure distributions for $A = 2.0$ flat delta wing at $\frac{x}{c_r} = 0.35$ , $\alpha = 20^\circ$ and $M = 0.9$ .....	16

LIST OF FIGURES - CONTINUED

<u>Figure</u>		<u>Page</u>
6	Effect of different types of modeling on spanwise pressure distributions for A = 2.0 flat delta wing at $\frac{x}{c_r} = 0.85$ , $\alpha = 20^\circ$ , and M = 0.9.....	18
7	Spanwise pressure distributions for A = 2.0 flat delta wing-body combination at $\alpha = 5^\circ$ and M = 0.7.....	20
8	Spanwise pressure distributions for A = 2.0 flat delta wing-body combination at $\alpha = 10^\circ$ and M = 0.7.....	21
9	Effect of fuselage on spanwise pressure distributions at $\frac{x}{c_r} = 0.35$ , $\alpha = 5^\circ$ , and M = 0.9.....	22
10	Effect of fuselage on spanwise pressure distributions at $\frac{x}{c_r} = 0.85$ , $\alpha = 5^\circ$ , and M = 0.9.....	23
11	Aerodynamic characteristics of A = 1.83 flat double delta wing at M = 0.9.....	24
12	Spanwise pressure distributions for A = 1.83 flat double delta wing at $\frac{x}{c_r} = 0.27$ , $\alpha = 5^\circ$ , and M = 0.9.....	25
13	Spanwise pressure distributions for A = 1.83 flat double delta wing at $\frac{x}{c_r} = 0.53$ , $\alpha = 5^\circ$ , and M = 0.9.....	26
14	Spanwise pressure distributions for A = 1.83 flat double delta wing at $\frac{x}{c_r} = 0.71$ , $\alpha = 5^\circ$ , and M = 0.9.....	27
15	Spanwise pressure distributions for A = 1.83 flat double delta wing at $\frac{x}{c_r} = 0.89$ , $\alpha = 5^\circ$ , and M = 0.9.....	28
16	Spanwise pressure distributions for A = 1.83 flat double delta wing at $\frac{x}{c_r} = 0.27$ , $\alpha = 10^\circ$ , and M = 0.9.....	29
17	Spanwise pressure distributions for A = 1.83 flat double delta wing at $\frac{x}{c_r} = 0.53$ , $\alpha = 10^\circ$ , and M = 0.9.....	30
18	Spanwise pressure distributions for A = 1.83 flat double delta wing at $\frac{x}{c_r} = 0.71$ , $\alpha = 10^\circ$ , and M = 0.9.....	31
19	Spanwise pressure distributions for A = 1.83 flat double delta wing at $\frac{x}{c_r} = 0.89$ , $\alpha = 10^\circ$ , and M = 0.9.....	32

LIST OF FIGURES - CONCLUDED

<u>Figure</u>		<u>Page</u>
20	Spanwise pressure distributions for A = 1.83 flat double delta wing at $\frac{x}{c_r} = 0.27$ , $\alpha = 15^\circ$ , and M = 0.9.....	33
21	Spanwise pressure distributions for A = 1.83 flat double delta wing at $\frac{x}{c_r} = 0.53$ , $\alpha = 15^\circ$ , and M = 0.9.....	34
22	Spanwise pressure distributions for A = 1.83 flat double delta wing at $\frac{x}{c_r} = 0.71$ , $\alpha = 15^\circ$ , and M = 0.9.....	35
23	Spanwise pressure distributions for A = 1.83 flat double delta wing at $\frac{x}{c_r} = 0.89$ , $\alpha = 15^\circ$ , and M = 0.9.....	36
<del>24</del>	DM-1 glider, with vertical fin removed and FLEE attached, modeled by FVS method.....	<del>37</del>
25	Velocity field for  at y = 0, and $\alpha = 6.16^\circ$ .....	38

STUDY OF HIGHLY SWEEPBACK WINGS BY THE  
FREE VORTEX SHEET METHOD

By

C. Subba Reddy<sup>1</sup> and Farhad Ghaffari<sup>2</sup>

ABSTRACT

The aerodynamic characteristics of highly sweptback wings with separation induced vortex flows have been numerically investigated using the free vortex sheet method, developed by Boeing Company, under a contract with NASA/Langley Research Center. The models studied included delta and straked wings, and wings with leading edge extensions. Also, PAN-AIR code has been used to design a fixed leading edge extension to a thick delta wing.

The theoretical results predicted have been compared with the experimental data wherever available, and the code capabilities and limitations explored. The fuselage effects on the aerodynamic performance have also been considered in some cases.

INTRODUCTION

This report briefly describes the research conducted under grant NSG 1561 during the period September 1, 1981 to August 15, 1982. In this work, the latest version of the free vortex sheet (FVS) method of Boeing Company (refs. 1 and 2) has been mainly employed to study various configurations not covered by the previous reports (refs. 3-6), with a view to determining the code capabilities and limitations. Also the recently incorporated code capability for modeling wings with multiple vortex systems has been utilized on double delta wings. The quasi-vortex lattice (QVL) method of Mehrotra (refs. 7 and 8) and the vortex lattice method with the suction analogy (VLM-SA) of NASA/Langley Research Center (refs. 9-11) which were extensively used in previous studies (refs. 3 and 4) have not been employed in this investigation. However, another code, PAN-AIR (ref. 12) has also been used to a

---

<sup>1</sup>Assistant Professor, Department of Mechanical Engineering and Mechanics, Old Dominion University, Norfolk, Virginia 23508.

<sup>2</sup>Research Assistant, Department of Mechanical Engineering and Mechanics, Old Dominion University, Norfolk, Virginia 23508.

limited extent. The models studied included thin delta and straked wings with fuselage attached. Also included are thick, and leading-edge flapped wings. The details of these planforms are given in table 1. In the following sections, the results are discussed and some of the code capabilities and limitations are evaluated.

#### NOMENCLATURE

A	aspect ratio
b	wing span
b(x)	local wing span
c	local wing chord
$\bar{c}$	mean aerodynamic chord
$c_r$	wing root chord
$C_D$	drag due-to-lift coefficient
$C_L$	lift coefficient
$C_m$	pitching moment coefficient
$\Delta C_p$	net lifting pressure coefficient
D	drag
FVS	free vortex sheet
M	Mach number
x,y,z	body axis coordinates
$\alpha$	angle of attack

#### RESULTS AND DISCUSSION

In this section, the results obtained by using the numerical codes are compared with the experimental data, wherever available, and the code capabilities and limitations are discussed. A summary of the configurations investigated is presented in table 1. The angle of attack range over which

the code is employed, the type of method used, and whether convergence is obtained or not, are also indicated in the table.

Figure 1 shows the delta and double delta wing models which are investigated using the FVS method (ref. 1). These are  $63.5^\circ$  delta and  $78.7^\circ/63.5^\circ$  double delta wings. The aerodynamic characteristics predicted by the method for the delta wing-body combination are compared with the experimental data (ref. 13) for various Mach numbers in figures 2-4. In figure 4, the results obtained for the wing only are also shown. As the figures indicate, the agreement between the predicted results and the data is not very good. In figures 5 and 6, the spanwise pressure distributions at two chordwise stations, obtained from different types of modeling of the delta wing by the FVS method, are compared with the experimental data. The data is not shown for the lower surface as it is not available. The predicted results and the data near the apex agree more favorably than they do near the trailing edge. In both cases, the predicted pressure peak is much higher than the actual one.

It is suggested in Boeing's instructional manual (ref. 2) that a carry-over lifting system, which extends the wing lifting system into the body, has to be used in order to model the body effects. However, when no carry over lifting system is used, the program still works and provides the results, which seem reasonable, for this wing as shown in figures 5 and 6. When the carry-over lifting system is used, it coincides with the upper body surface because the body exists only on the underside of the wing. The pressure values obtained from this model are unrealistic on and near the body as can be seen from the figures. Therefore, this type of modeling has not been used in further investigations. However, when the carry-over lifting system and the upper body surface are separated by a small distance (0.01 compared to  $C_r = 250$ ) by lifting up the upper body surface, the results are dramatically improved. The results obtained by this modeling, and the modeling without any carry-over system, are essentially the same as shown by the figures. However, the solution convergence is faster and, hence, less computational time is needed in the case of modeling with no carry-over lifting system. Therefore, throughout this work, this type of modeling has been used whenever the body effects are to be included.



Figures 7-10 show the spanwise pressure distributions at various chordwise stations, angles of attack and Mach numbers. Experimental data is compared with the predicted results, wherever available, and found that there is not a good agreement between them in the outboard region of the wing.

The 78.7°/63.5° double delta wing is modeled using two separate vortex systems on inboard and outboard leading edges. The predicted longitudinal aerodynamic characteristics compare favorably with the experimental results, as indicated by figure 11. Spanwise pressure distributions at different locations for various angles of attack are illustrated in figures 12 to 23. The predicted pressure distribution on the forward portion of the wing, before the break in the leading edge occurs, agrees reasonably well with the experimental data; in the aft portion, the agreement is comparatively not good. However, the method predicts the two pressure peaks as the data shows.

A thick, round-edged delta wing glider, also called DM-1 (ref. 14), was originally studied in 1946 with the aim of developing a supersonic airplane. The DM-1 glider has approximately a delta planform and NACA-0015-64 airfoil sections with an aspect ratio of 1.8 and a 60° swept-back leading edge.

The flat DM-1 glider with Flat Leading Edge Extension (FLEE) and vertical fin removed, is modeled by the FVS method (ref. 1) as shown in figure 24. The aerodynamic characteristics obtained are compared with the data at  $\alpha = 15^\circ$  and  $M = 0.0$  in table 2. Further investigation of DM-1 using the FVS method is in progress.

Another thick wing with camber and twist is being investigated using PAN-AIR CODE (ref. 12) for design purposes. The objective of this study is to develop the technology by which a Fixed Leading Edge Extension (FLEE) can be added to a wing without affecting its performance at cruise. The FLEE device, to be designed, would lie along the stagnation stream surface for the wing at its cruise angle of attack. At angles of attack greater than for the cruise, vertical flows would be generated by the device and based on

the results for the DM-1 glider the increase in drag can be minimized. For this purpose the flow fields at different spanwise stations are analyzed and stagnation points and surfaces determined. Such analysis is shown in figure 25 for a particular airfoil section at the wing root and for a designed angle of attack of  $6.16^\circ$ . Further investigation of this study is in progress.

#### CONCLUSIONS

The aerodynamics performance of low-aspect ratio sweptback wings with vortex flows has been investigated using a numerical code, developed by Boeing Company, and sponsored by NASA/Langley Research Center. Wings of different planforms have been studied and the predicted results compared to the existing data, wherever possible, in order to determine the code capabilities and limitations. Another Boeing Company code, PAN-AIR, has also been used to develop a fixed leading edge extension to a thick delta wing.

The longitudinal aerodynamic characteristics predicted by the free vortex sheet method for the delta wing-body combination do not compare favorably with the data. However, there is a fairly good agreement in the case of a double delta wing with no fuselage effects considered. Also the method provides results for the above delta wing with no body effects considered which agree better with the data than those when the body is included.

In the case of spanwise pressure distributions, the predicted results and the data agree more favorably near the apex than they do near the trailing edge. However, in both cases, the predicted pressure peak values are higher than the actual ones. The method with double vortex modeling predicts two pressure peaks as the data shows in the case of double delta wing.

## REFERENCES

1. Johnson, F.T.; Lu, P.; Tinoco, E.N.; and Epston, M.A.: An Improved Panel Method for the Solution of Three-Dimensional Leading-Edge Vortex Flows. Volume I - Theory Document. NASA CR-3278, 1980.
2. Tinoco, E.T.; Lu, P.; and Johnson, F.T.: An Improved Panel Method for the Solution of Three-Dimensional Leading-Edge Vortex Flows. Volume II - User's Guide and Programmer's Document. NASA CR-3279, 1980.
3. Reddy, C.S.: Theoretical Study of Aerodynamic Characteristics of Wings Having Vortex Flow. NASA CR-159184, 1979.
4. Reddy, C.S.: Investigation of Aerodynamic Characteristics of Wings Having Vortex Flow Using Different Numerical Codes. NASA CR-165706, 1981.
5. Reddy, C.S.: Numerical Study of Aerodynamic Characteristics of Swept-back Wings Having Vortex Flows. Progress Report for NASA Grant NSG 1561, 1980.
6. Reddy, C.S.: Aerodynamic Performance of Slender Wings with Separated Flows. Technical Report, Old Dominion University Research Foundation, Norfolk, VA, 1982.
7. Mehrotra, S.C.: A Theoretical Investigation of the Aerodynamics of Low Aspect-Ratio Wings with Partial Leading-Edge Separation. NASA CR-145304, 1978.
8. Mehrotra, S.C.; and Lan, C.E.: A Computer Program for Calculating Aerodynamic Characteristics of Low-Aspect Ratio Wings with Partial Leading-Edge Separation. NASA CR-145362, 1978.
9. Polhamus, E.C.: A Concept of the Vortex Lift of Sharp-Edge Delta Wings Based on a Leading-Edge Suction Analogy. NASA TN D-3767, 1966.
10. Margason, R.J.; and Lamar, J.E.: Vortex-Lattice Fortran Program for Estimating Subsonic Aerodynamic Characteristics of Complex Planforms. NASA TN-D-6142, 1971.
11. Lamar, J.E.; and Gloss, B.B.: Subsonic Aerodynamic Characteristics of Interacting Lifting Surfaces with Separated Flow Around Sharp Edges Predicted by a Vortex-Lattice Method. NASA TN D-7921, 1975.
12. Sidwek, K.W.; Baruah, P.K.; and Bussoletti: PAN-AIR A Computer Program for Predicting Subsonic or Supersonic Linear Potential Flows About Arbitrary Configurations Using a Higher Order Panel Method. NASA CR 3252, 1980.

13. Stahl, W.: On the Effect of Strake on the Flow Field of a Delta Wing ( $\Lambda = 2$ ) at Near-Sonic Velocities. N76-11052 (A Reproduced Copy for NASA), 1965.
  
14. Wilson, Jr. H.A.; and Lovell, J.C.: Full-Scale Investigation of the Maximum Lift and Flow Characteristics of an Airplane Having Approximately Triangular Planform. NACA RM No. LGK20, 1947.

Table 1. Wing configurations modeled by the FVS method.

<u>Wing Description</u>	<u>Modeling Details</u>	<u>Angle of Attack</u>	<u>Mach Number</u>	<u>Method of Solution</u>	<u>Solution Converged?</u>
63.5° flat delta wing, A = 2.0	Without near wake	5-20°	0.9	Quasi-Newton	yes
63.5° flat delta wing-body combination, A = 2.0	Without near wake or carry-over lifting system	5°,10°	0.5,0.7	Quasi-Newton	yes
63.5° flat delta wing-body combination, A = 2.0	Without near wake or carry-over lifting system	5°-20°	0.9	Quasi-Newton	yes
63.5° flat delta wing-body combination, A = 2.0	With near wake, and without carry-over lifting system	5°	0.9	Quasi-Newton and Least Squares	no
63.5° flat delta wing-body combination, A = 2.0	Without near wake, and with carry-over lifting system coinciding with upper body surface	20°	0.9	Quasi-Newton	yes
63.5° flat delta wing-body combination, A = 2.0	Without near wake, and with carry-over lifting system and the upper body surface separated by a small distance (0.01); discontinuity exists between body and wing upper surfaces	20°	0.9	Quasi-Newton	yes

Table 1. (Continued).

<u>Wing Description</u>	<u>Modeling Details</u>	<u>Angle of Attack</u>	<u>Mach Number</u>	<u>Method of Solution</u>	<u>Solution Converged?</u>
63.5° flat delta wing-body combination, A = 2.0	Without near wake, and with carry-over lifting system and the upper body surface separated by a small distance (0.01); no discontinuity exists between body and wing upper surfaces	20°	0.9	Quasi-Newton	yes
78.7°/63.5° flat double delta wing; A = 1.83	Without near wake, and with single vortex system along inboard leading edge only	20°	0.9	Quasi-Newton	yes
78.7°/63.5° flat double delta wing; A = 1.83	Without near wake, and with single vortex system all along leading edge	20°	0.9	Quasi-Newton	yes
78.7°/63.5° flat double delta wing; A = 1.83	Without near wake, and with two separate vortex systems along inboard and outboard leading edges	20°	0.9	Quasi-Newton	no
78.7°/63.5° flat double delta wing; A = 1.83	Without near wake, and with two separate vortex systems along inboard and outboard leading edges	5°-20°	0.9	Least Squares	yes

Table 1. (Concluded).

<u>Wing Description</u>	<u>Modeling Details</u>	<u>Angle of Attack</u>	<u>Mach Number</u>	<u>Method of Solution</u>	<u>Solution Converged?</u>
78.7°/63.5° flat double delta wing body combination, A = 1.83	Without near wake or carry-over lifting system, and with single vortex all along leading edge	20°	0.9	Least Squares	no
78.7°/63.5° flat double delta wing-body combination A = 1.83	Without near wake, or carry-over lifting system, and with two separate-vortex systems along inboard and outboard leading edges	20°	0.9	Least Squares	no
60° flat delta (DM-1 glider with thickness neglected) with flat leading edge extension, A = 1.8	With near wake	15°	0	Quasi-Newton	no
60° flat delta (DM-1 glider with thickness neglected) with flat leading edge extension, A = 1.8	With near wake	15°	0	Least Squares	yes (but convergence is slow and not very good)

Table 2. Comparison of aerodynamic characteristics of DM-1 glider at  $\alpha = 15^\circ$  and  $M = 0$ .

<u>Method</u>	<u>C<sub>L</sub></u>	<u>C<sub>D</sub></u>	<u>C<sub>m</sub></u>
FVS method	0.68	0.18	0.010
Data (ref. 14)	0.55	0.12	-0.038



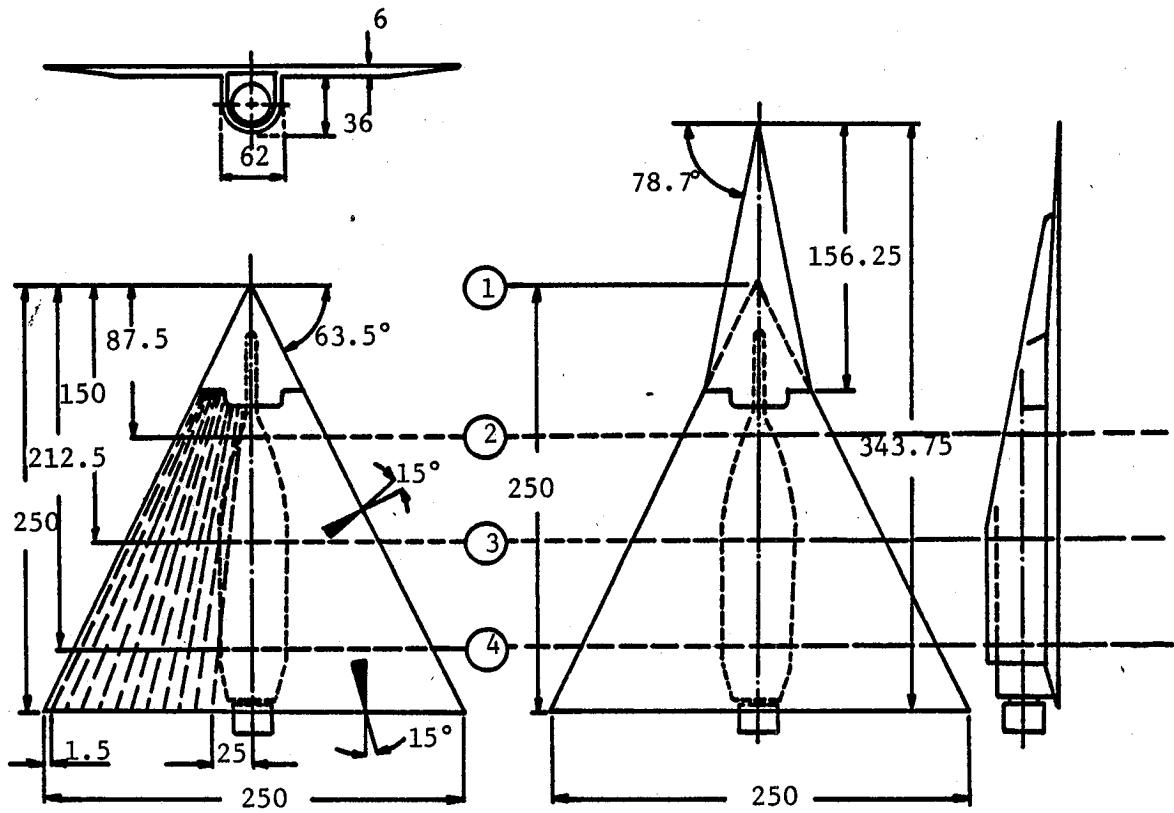


Figure 1. Geometry and principal dimensions of delta and double delta wing models.



DATA (Ref. 13)



FVS METHOD (Ref. 1)

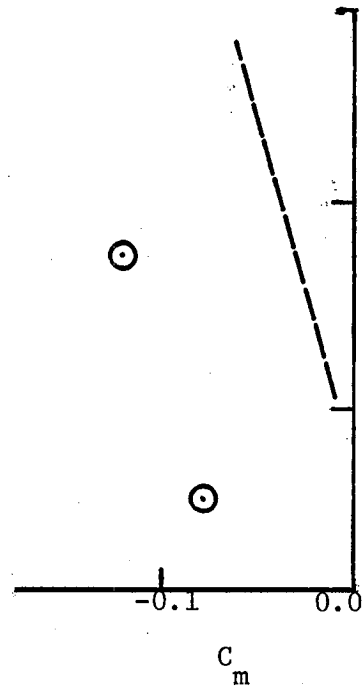
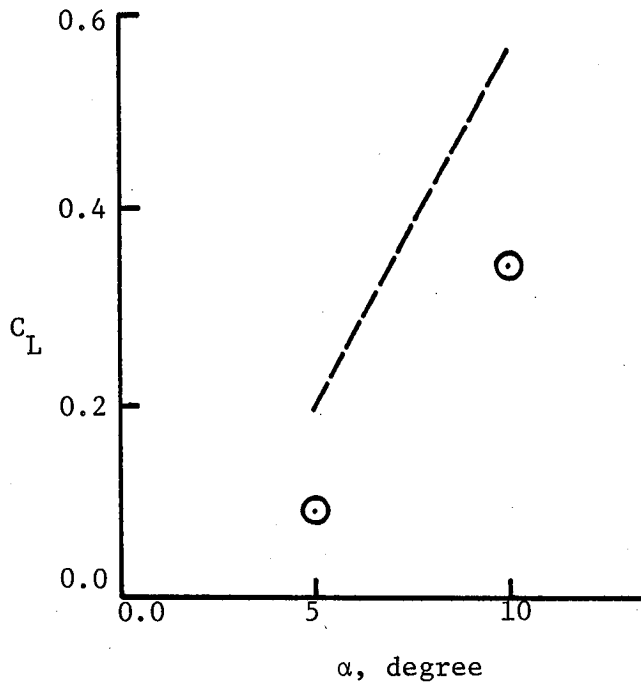
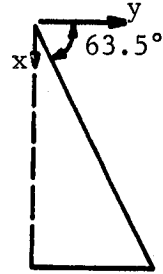


Figure 2. Aerodynamic characteristics of  $A = 2.0$  flat delta wing-body combination at  $M = 0.5$ .

⊙ DATA (Ref. 13)

----- FVS METHOD (Ref. 1)

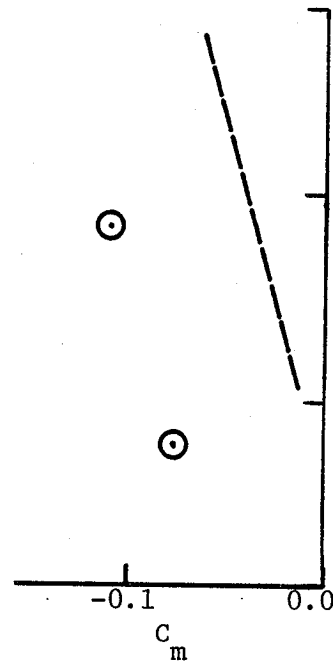
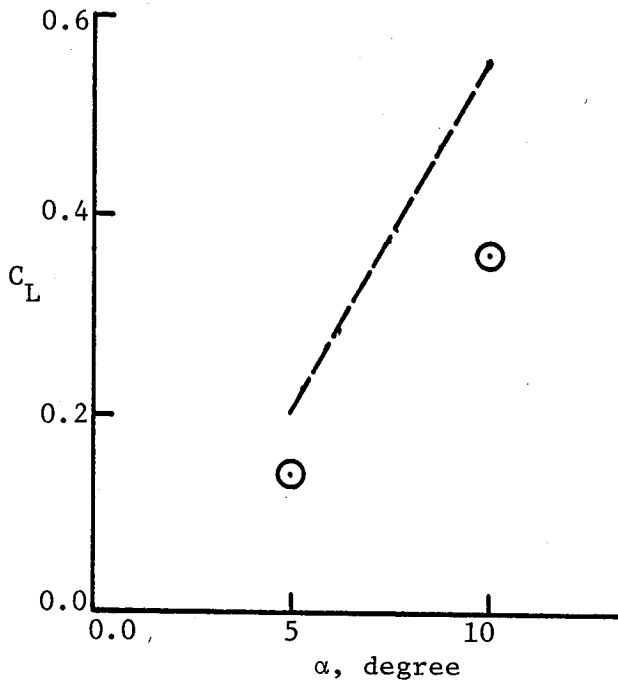
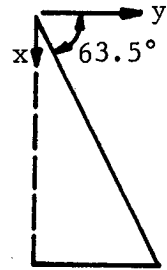


Figure 3. Aerodynamic characteristics of  $A = 2.0$  flat delta wing-body combination at  $M = 0.7$ .

○ DATA (Ref. 13)  
 - - - WING-BODY COMBINATION  
 ——— WING ONLY

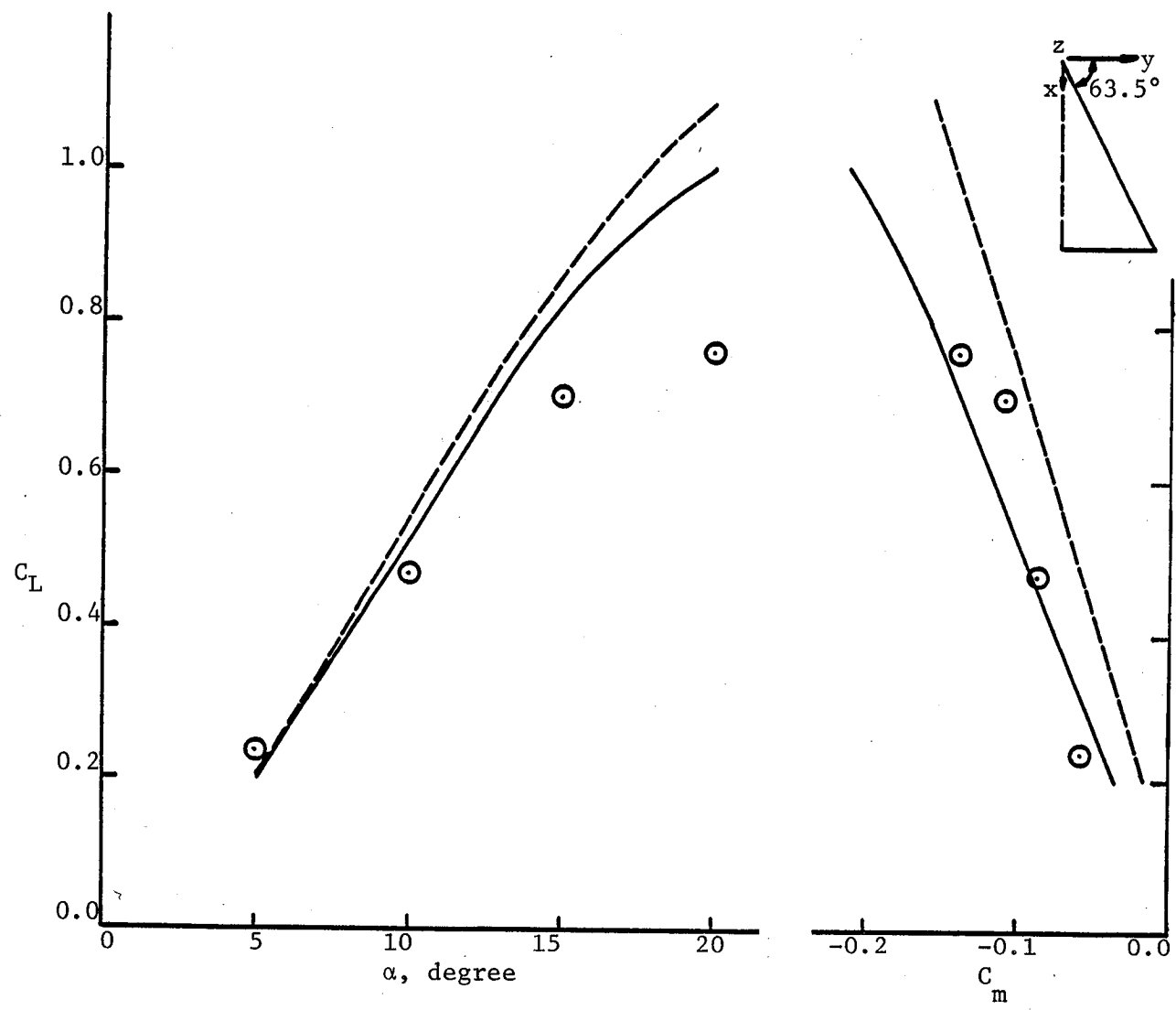
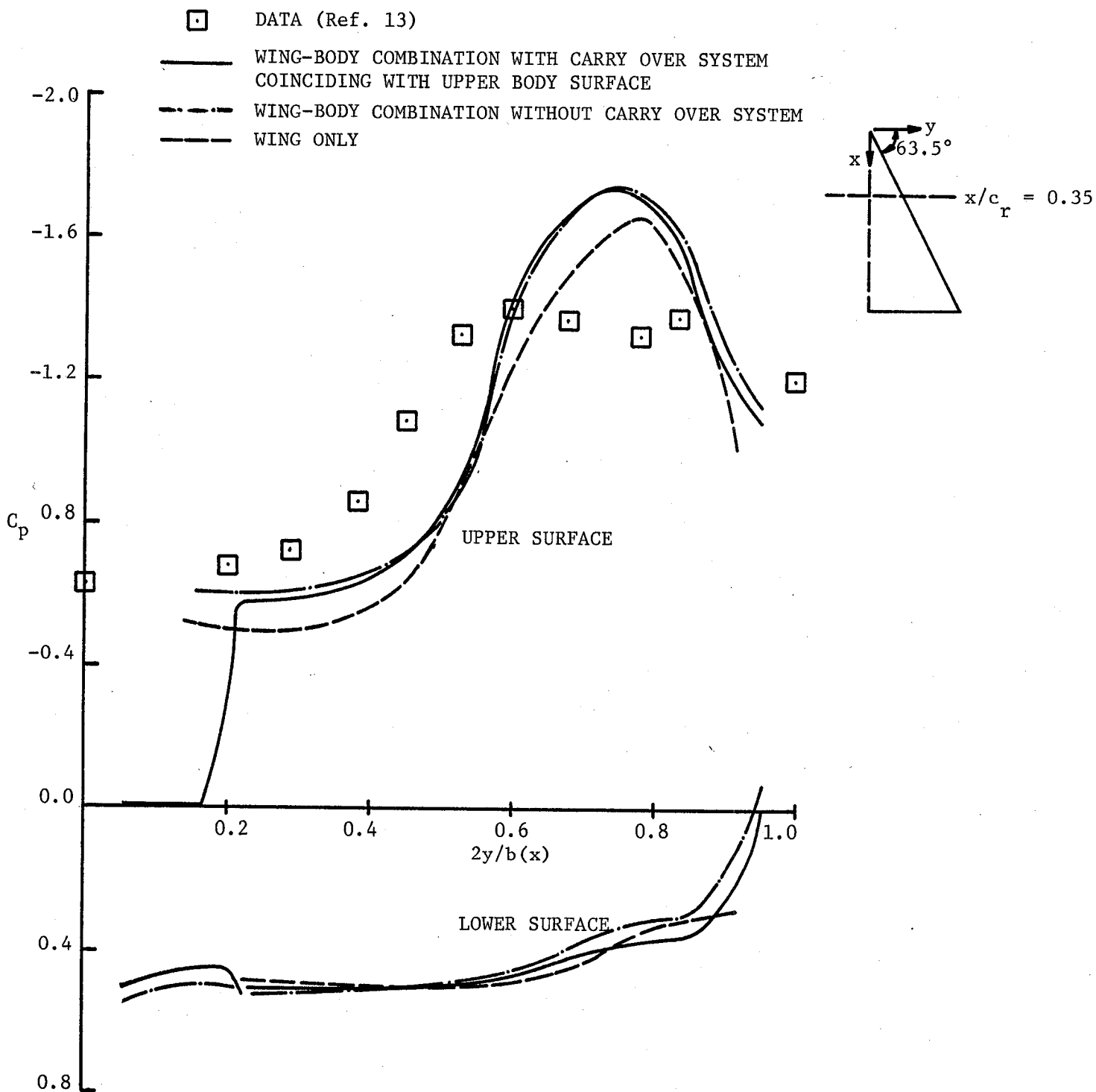


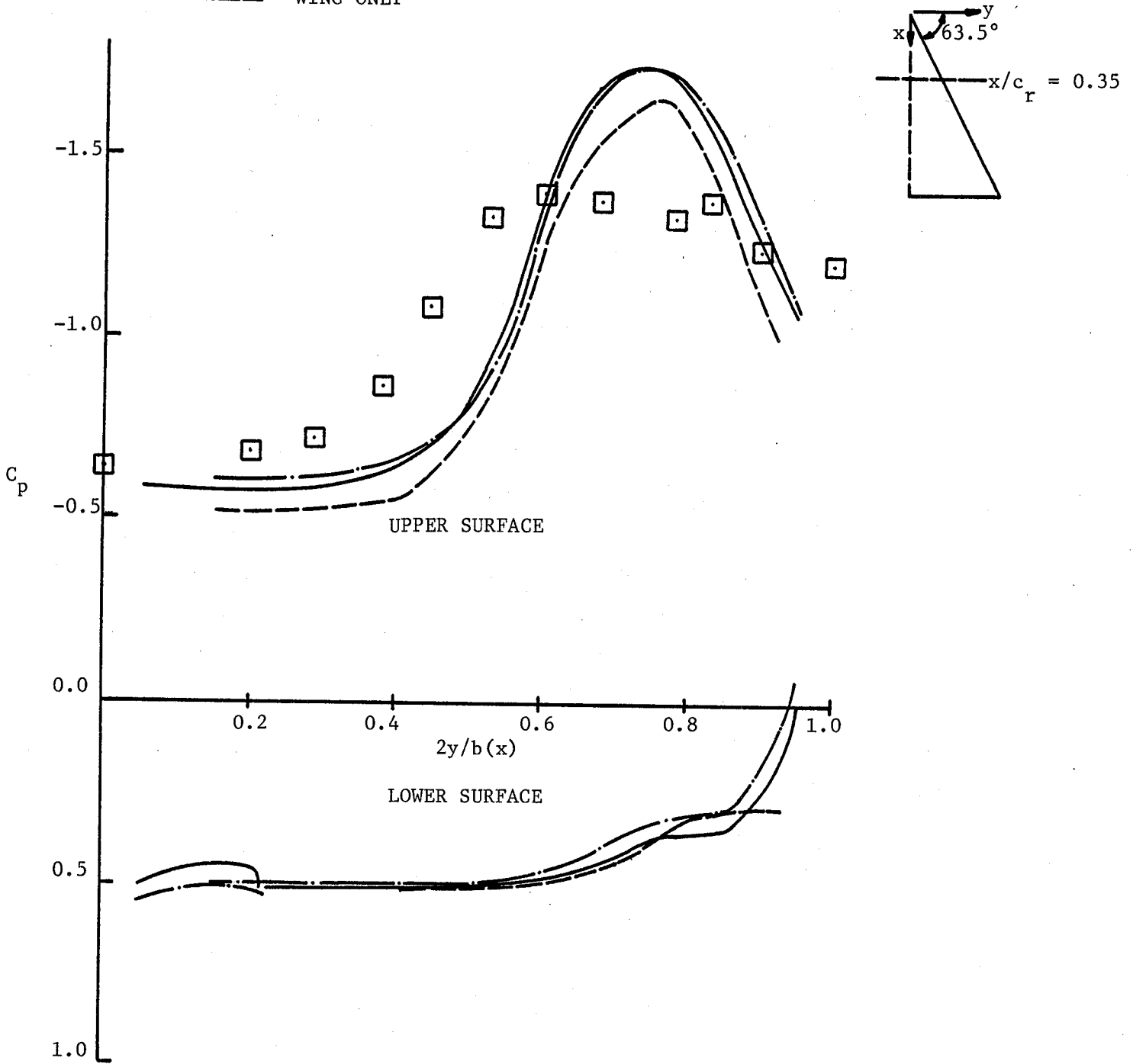
Figure 4. Aerodynamic characteristics of  $A = 2.0$  flat delta wing-body combination at  $M = 0.9$ .



(a)

Figure 5. Effect of different types of modeling on spanwise pressure distributions for  $A = 2.0$  flat delta wing at  $\frac{x}{c_r} = 0.35$ ,  $\alpha = 20^\circ$ , and  $M = 0.9$ .

- DATA (Ref. 13)
- WING-BODY COMBINATION WITHOUT CARRY OVER SYSTEM SEPARATED FROM UPPER BODY SURFACE BY A SMALL DISTANCE
- - - WING-BODY COMBINATION WITHOUT CARRY OVER SYSTEM
- - - WING ONLY



(b)

Figure 5. Concluded.

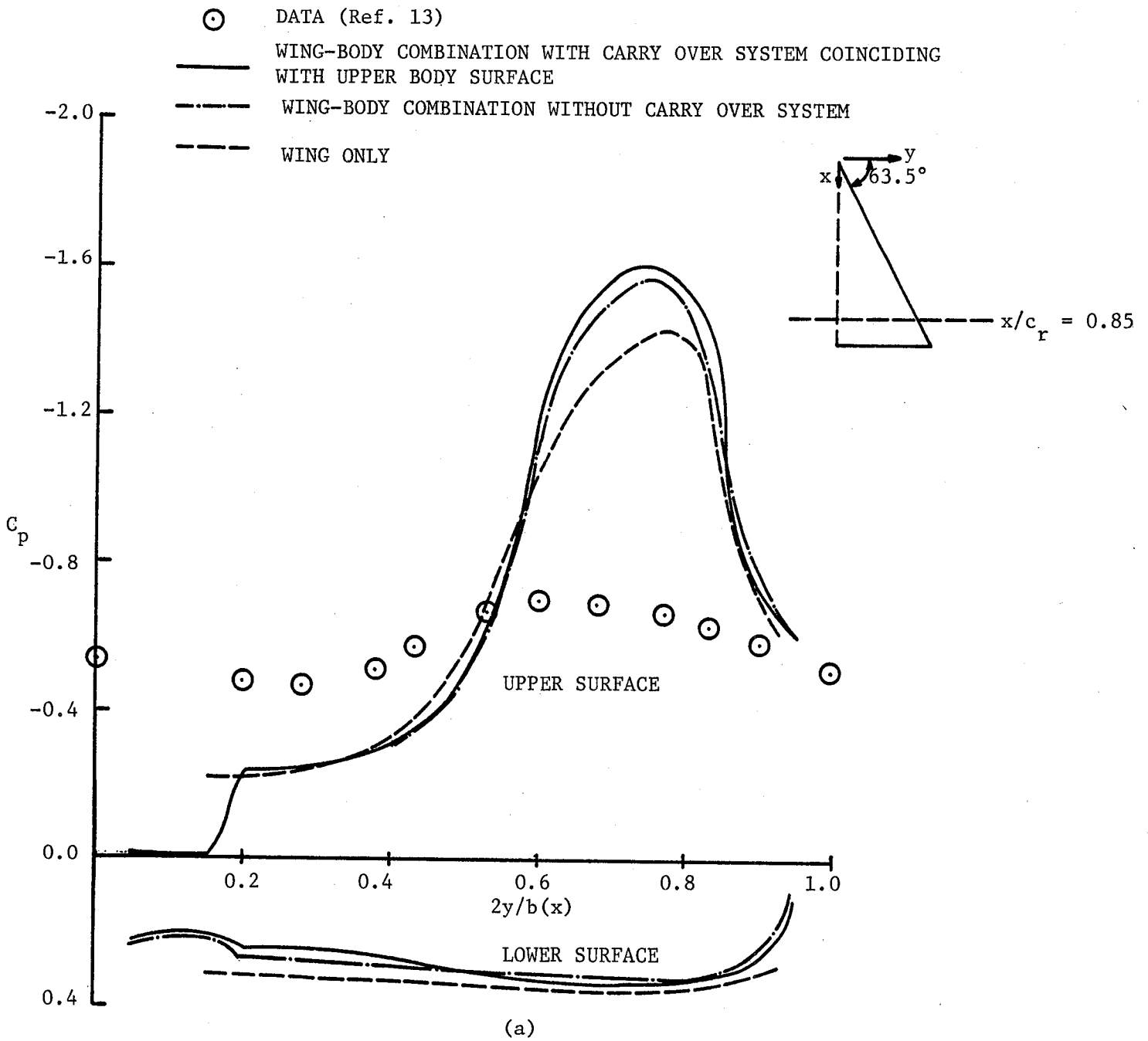
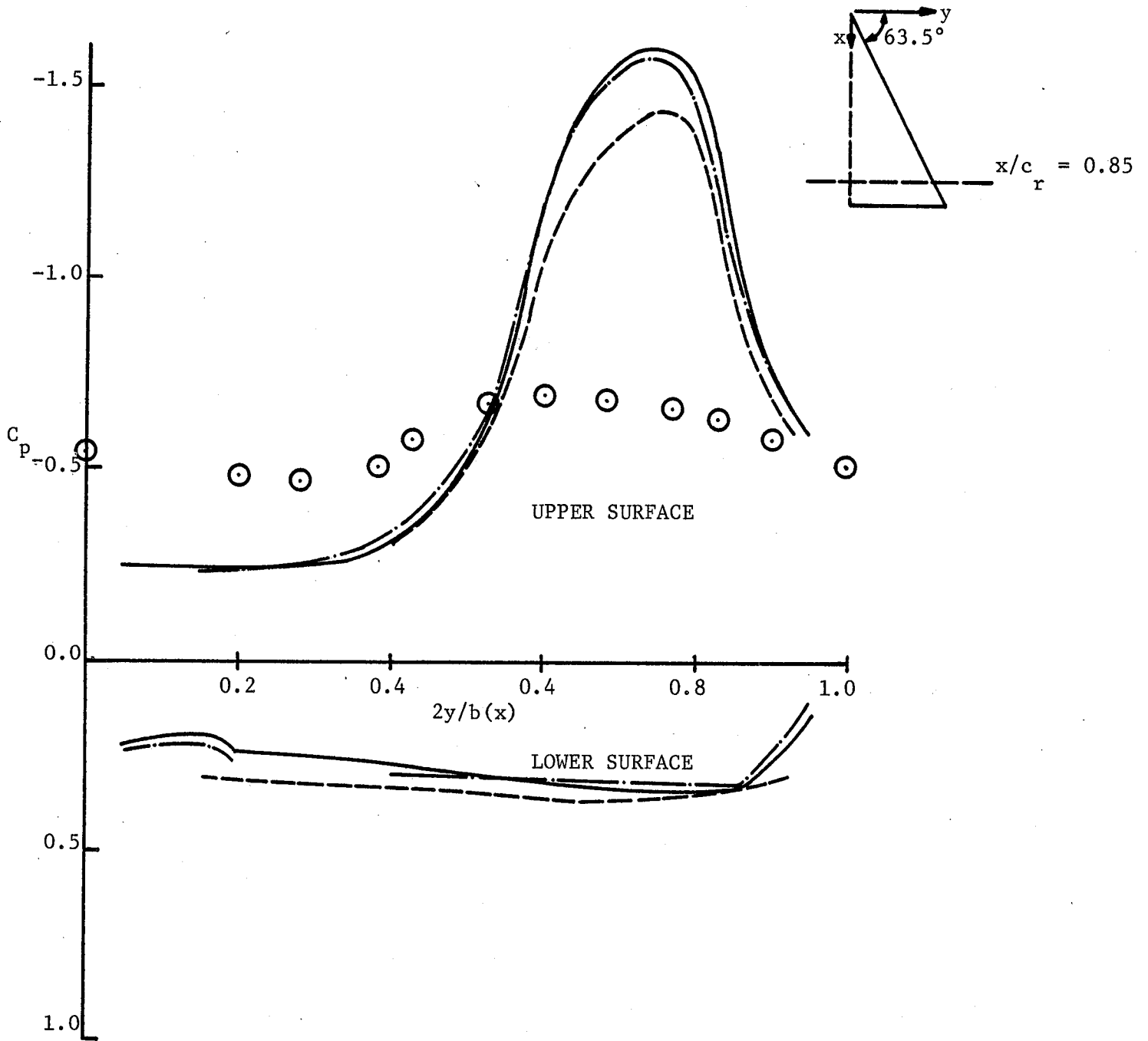


Figure 6. Effect of different types of modeling on spanwise pressure distributions for  $A = 2.0$  flat delta wing at  $\frac{x}{c_r} = 0.85$ ,  $\alpha = 20^\circ$ , and  $M = 0.9$ .

- DATA (Ref. 13)
- WING-BODY COMBINATION WITH CARRY OVER SYSTEM  
SEPARATED FROM UPPER BODY SURFACE BY A SMALL DISTANCE
- · - · WING-BODY COMBINATION WITHOUT CARRY OVER SYSTEM
- - - WING ONLY



(b)

Figure 6. Concluded.



- · - · -  $x/c_r = 0.35$   
 - - - -  $x/c_r = 0.85$

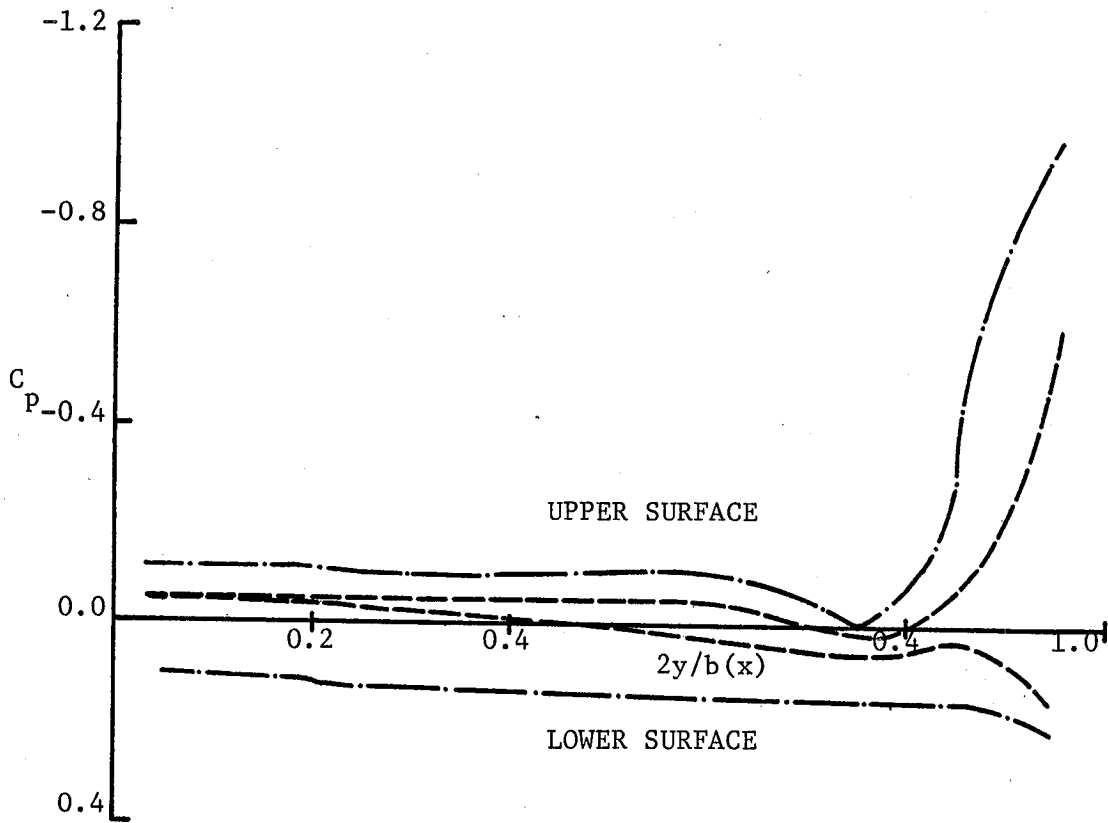
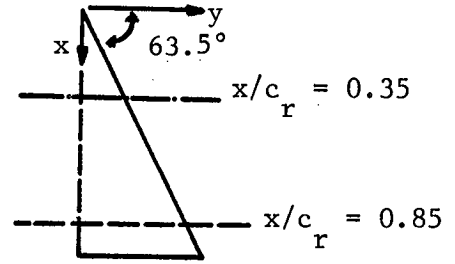


Figure 7. Spanwise pressure distributions for  $A = 2.0$  flat delta wing-body combination at  $\alpha = 5^\circ$  and  $M = 0.7$ .

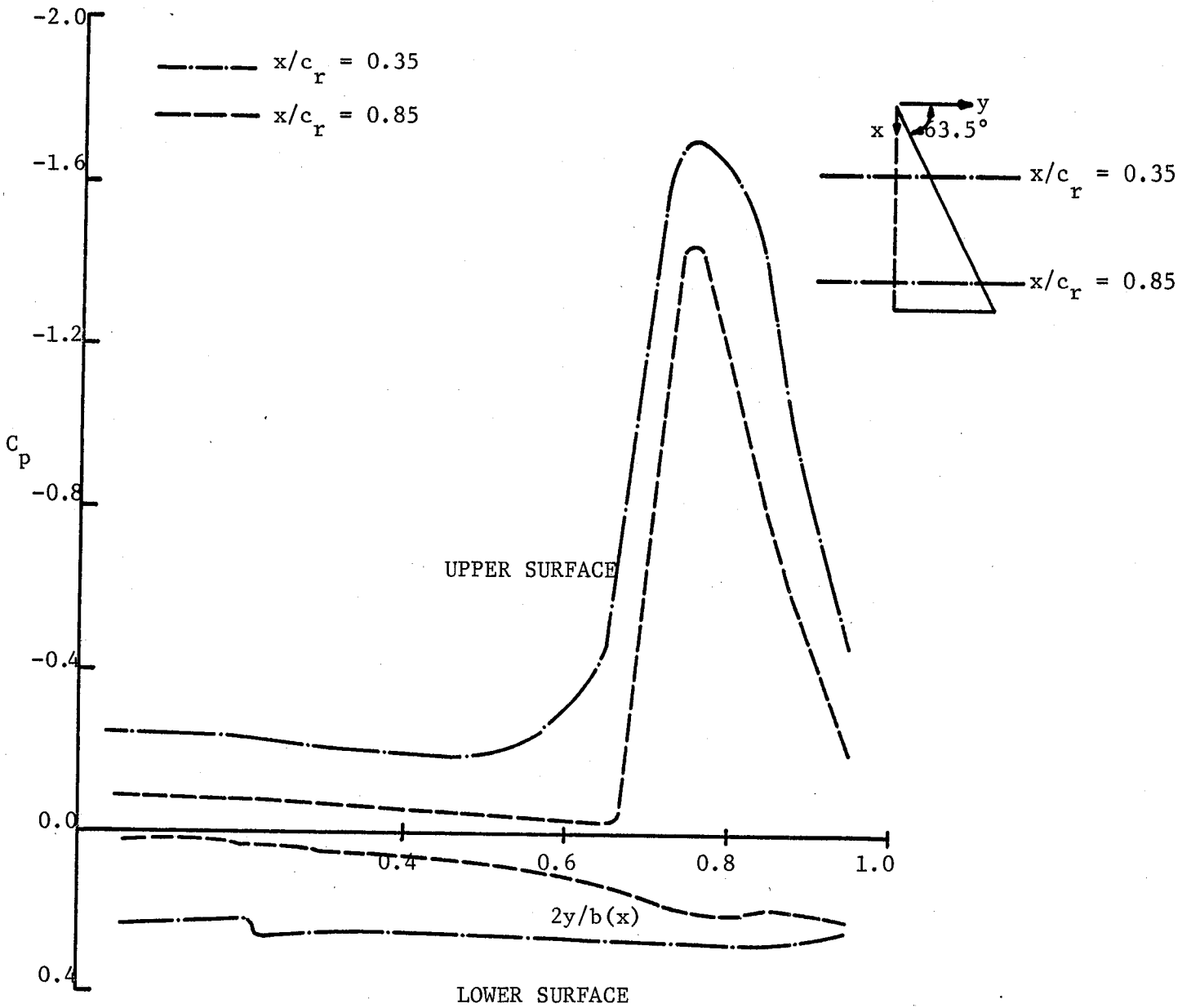


Figure 8. Spanwise pressure distributions for  $A = 2.0$  flat delta wing-body combination at  $\alpha = 10^\circ$  and  $M = 0.7$ .

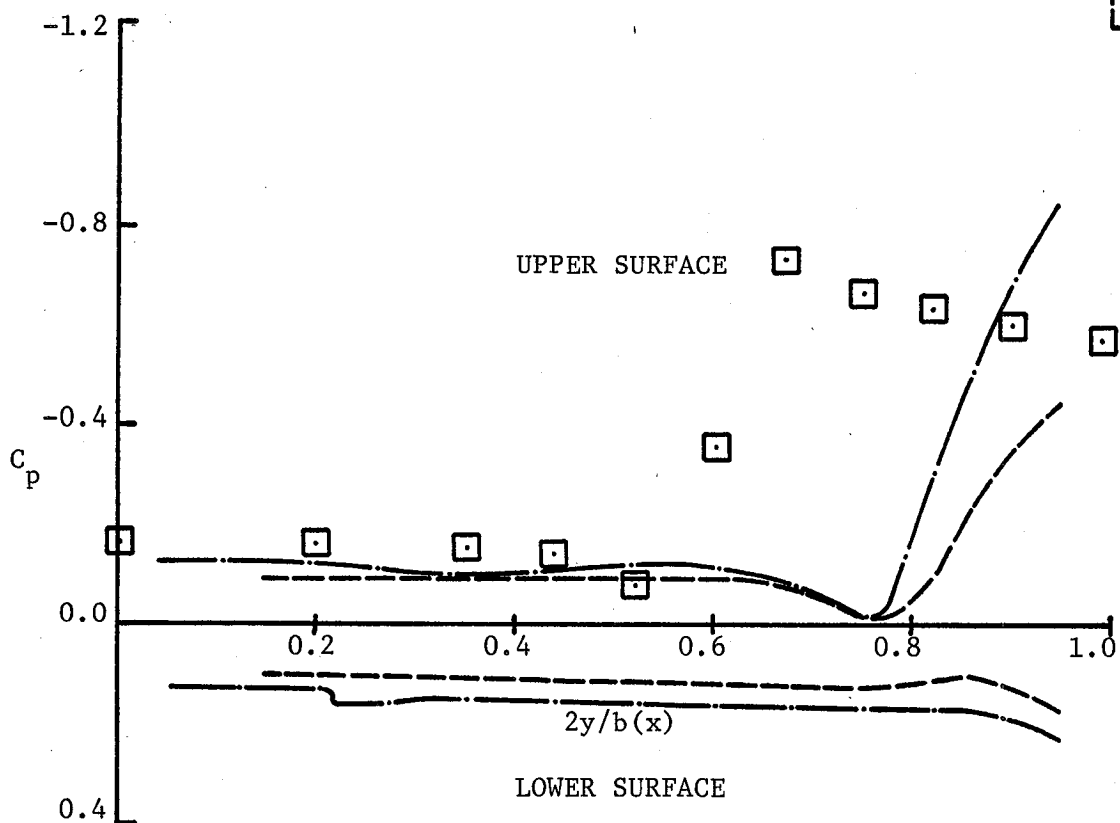
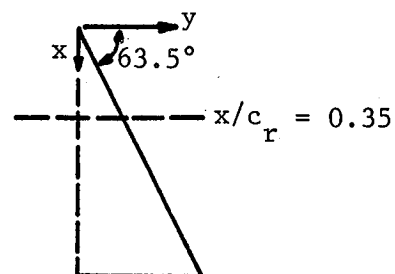
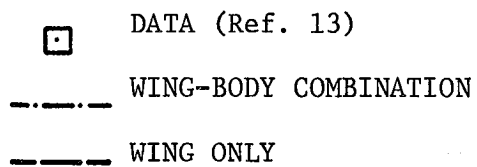


Figure 9. Effect of fuselage on spanwise pressure distributions  $\frac{x}{c_r} = 0.35$ ,  $\alpha = 5^\circ$ , and  $M = 0.9$ .

○ DATA (Ref. 13)  
 - · - · - WING-BODY COMBINATION  
 - - - WING ONLY

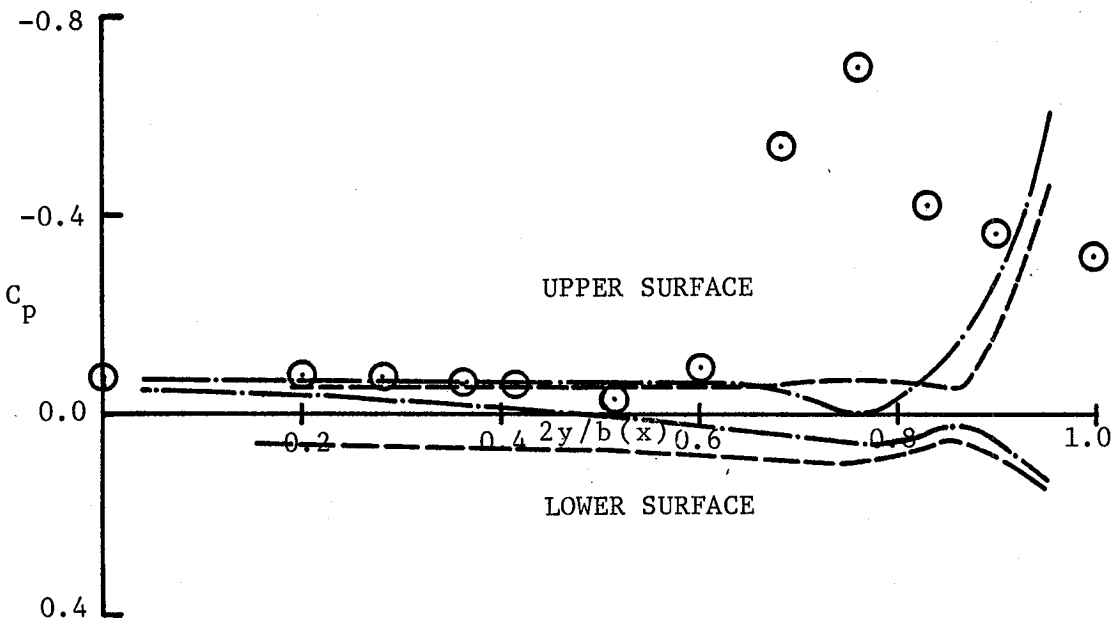
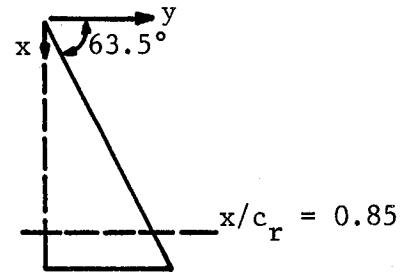


Figure 10. Effect of fuselage on spanwise pressure distributions  $\frac{x}{c_r} = 0.85$ ,  $\alpha = 5^\circ$ , and  $M = 0.9$ .

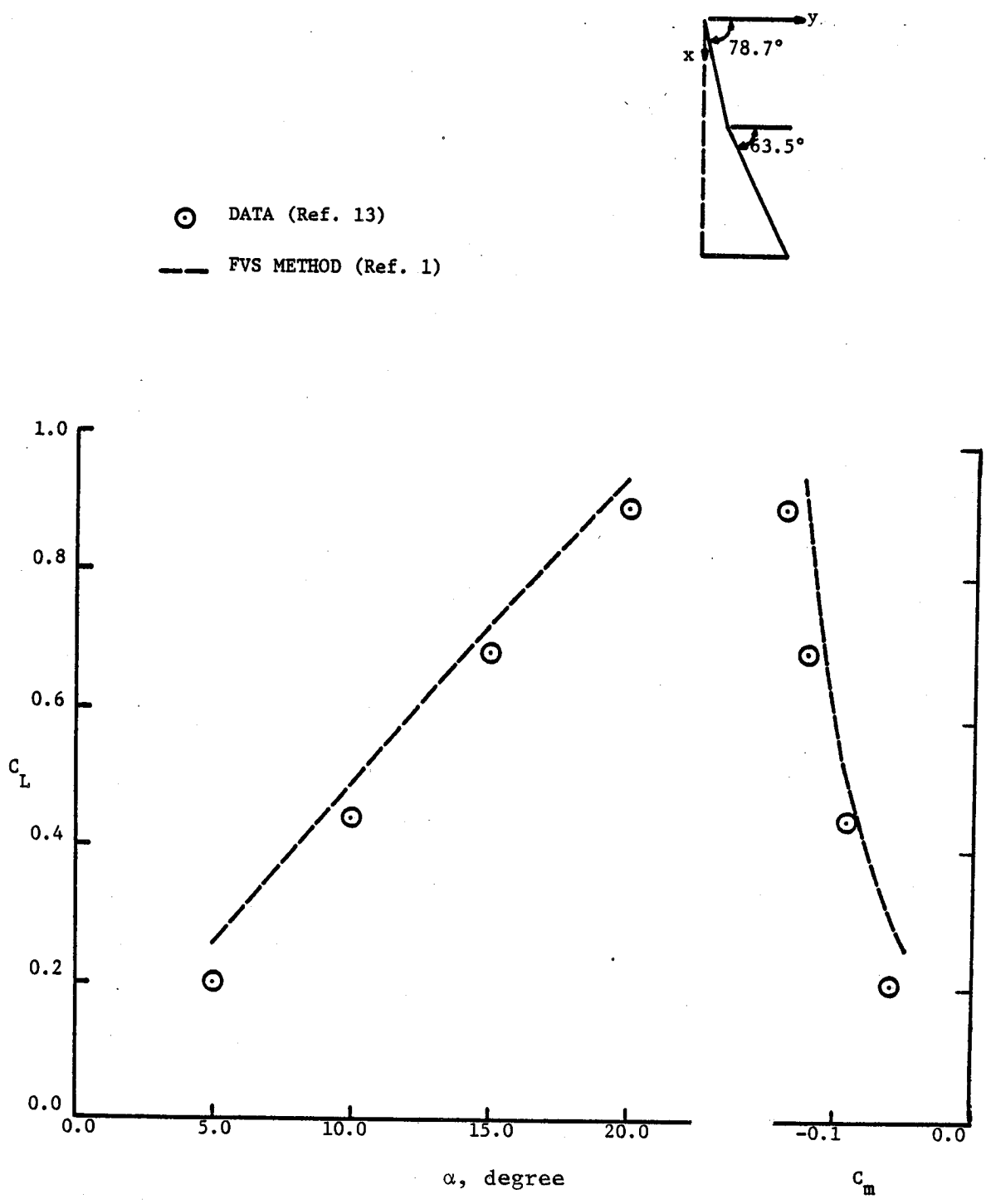
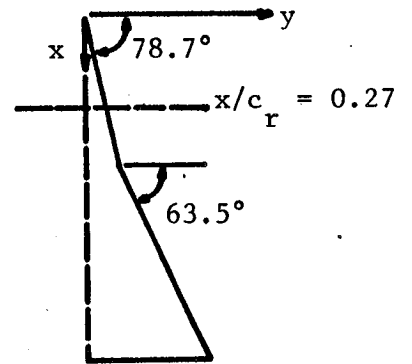


Figure 11. Aerodynamic characteristics of  $A = 1.83$  flat double delta wing at  $M = 0.9$ .



○ DATA (Ref. 13)  
 - - - FVS METHOD (Ref. 1)

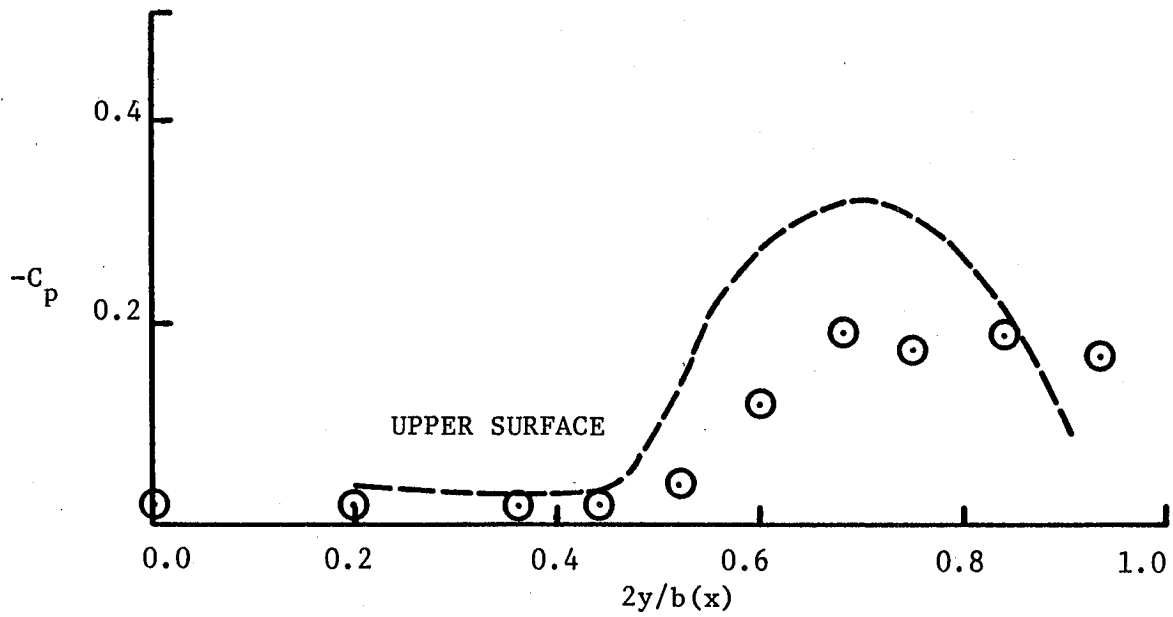


Figure 12. Spanwise pressure distributions for  $A = 1.83$  flat double delta wing at  $\frac{x}{c_r} = 0.27$ ,  $\alpha = 5^\circ$ , and  $M = 0.9$ .

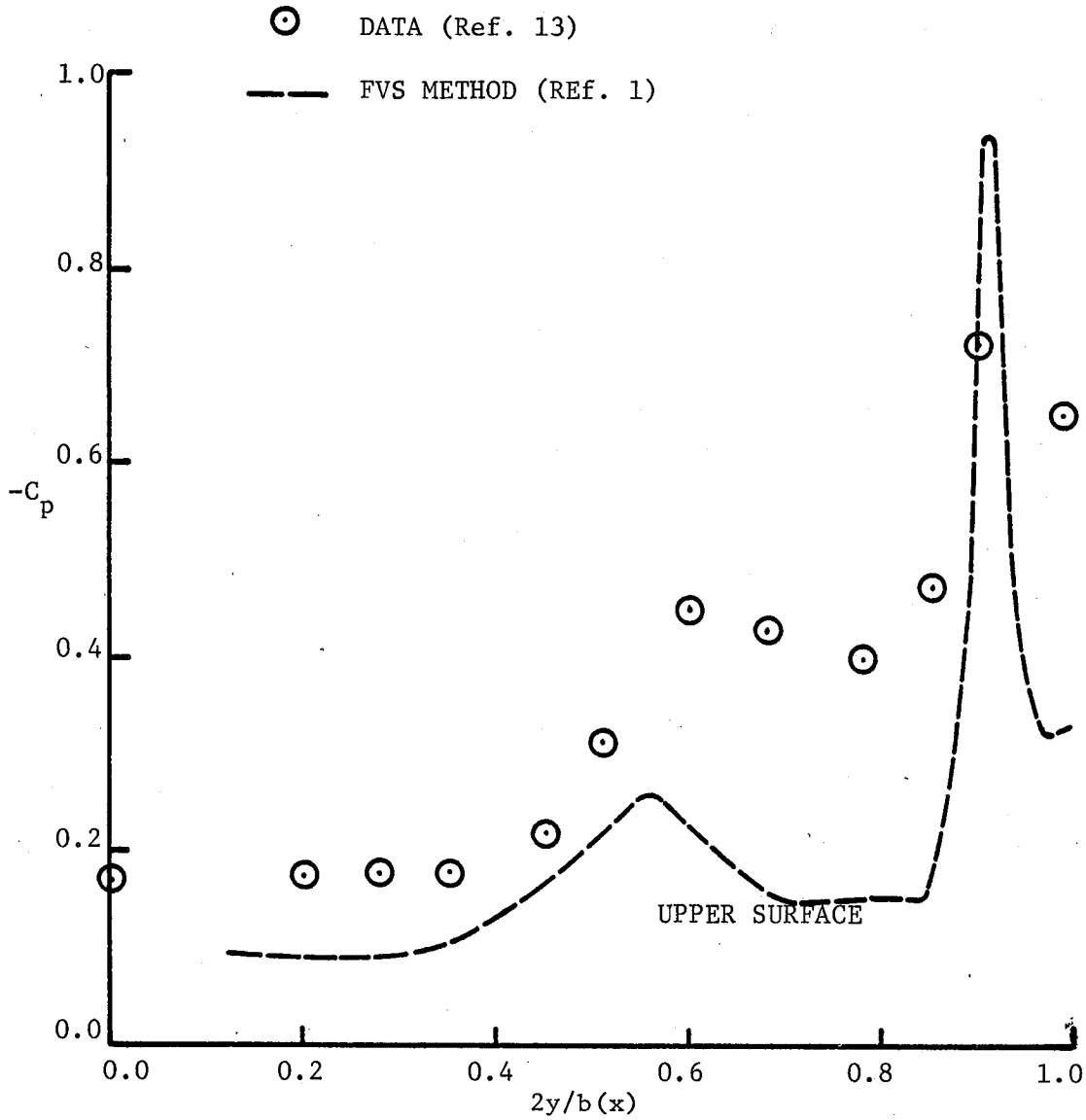
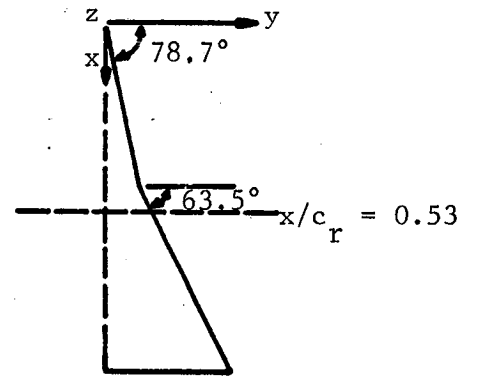
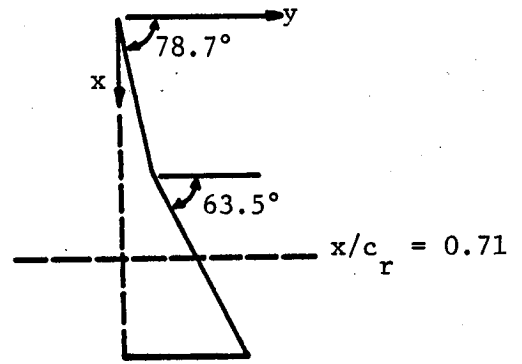


Figure 13. Spanwise pressure distributions for  $A = 1.83$  flat double delta wing at  $\frac{x}{c_r} = 0.53$ ,  $\alpha = 5^\circ$ , and  $M = 0.9$ .



○ DATA (Ref. 13)  
 - - - FVS METHOD (Ref. 1)

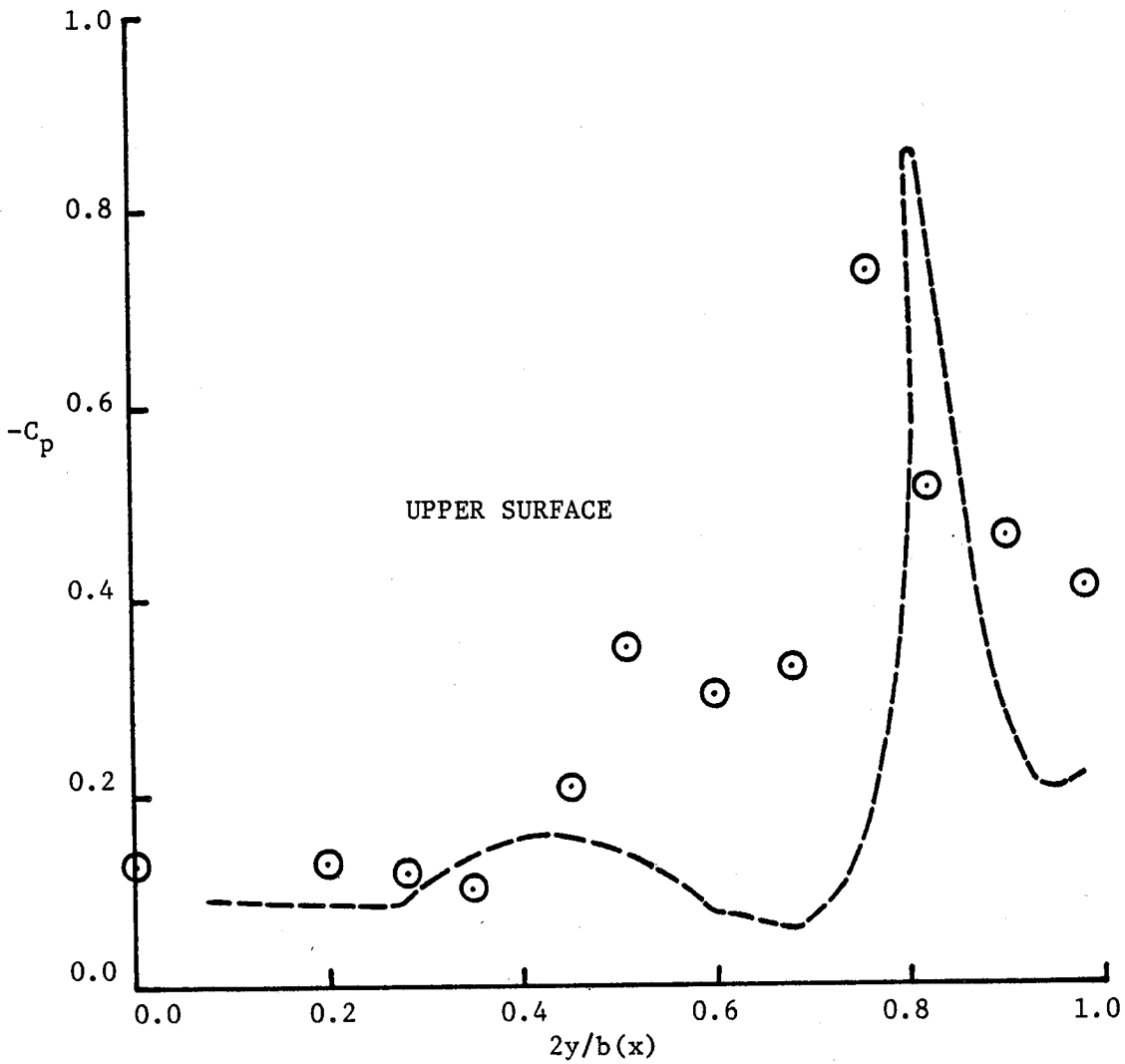


Figure 14. Spanwise pressure distributions for  $A = 1.83$  flat double delta wing at  $\frac{x}{c_r} = 0.71$ ,  $\alpha = 5^\circ$ , and  $M = 0.9$ .



○ DATA (Ref. 13)  
 - - - FVS METHOD (Ref. 1)

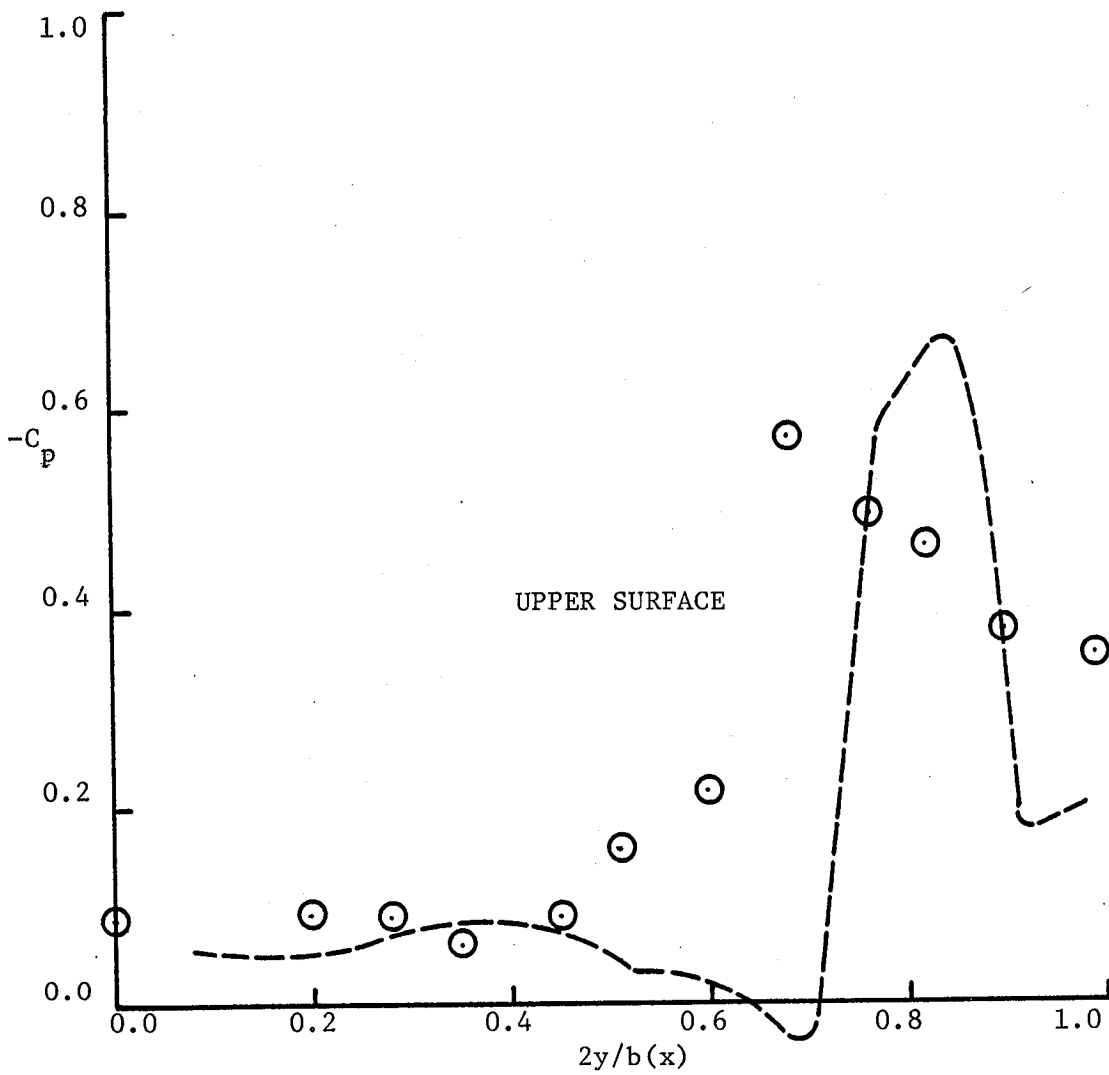
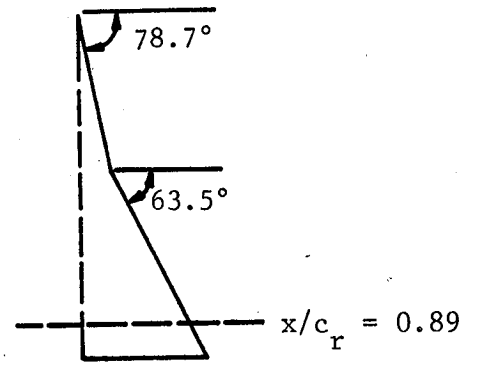
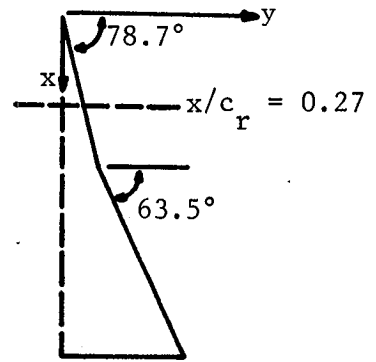


Figure 15. Spanwise pressure distributions for  $A = 1.83$  flat double delta wing at  $\frac{x}{c_r} = 0.89$ ,  $\alpha = 5^\circ$ , and  $M = 0.9$ .



⊙ DATA (Ref. 13)

--- FVS METHOD (Ref. 1)

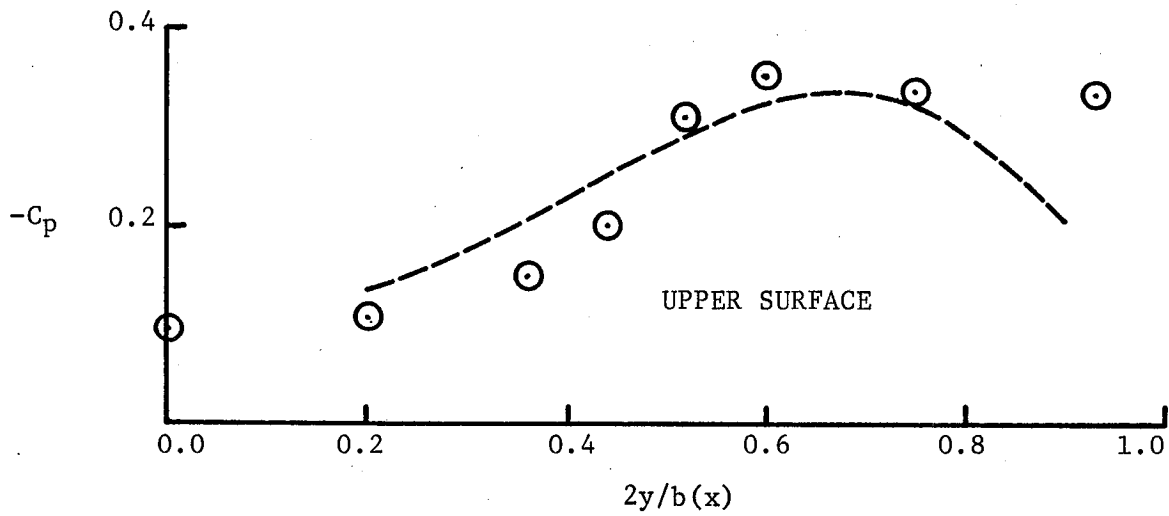


Figure 16. Spanwise pressure distributions for  $A = 1.83$  flat double delta wing at  $\frac{x}{c_r} = 0.27$ ,  $\alpha = 10^\circ$ , and  $M = 0.9$ .

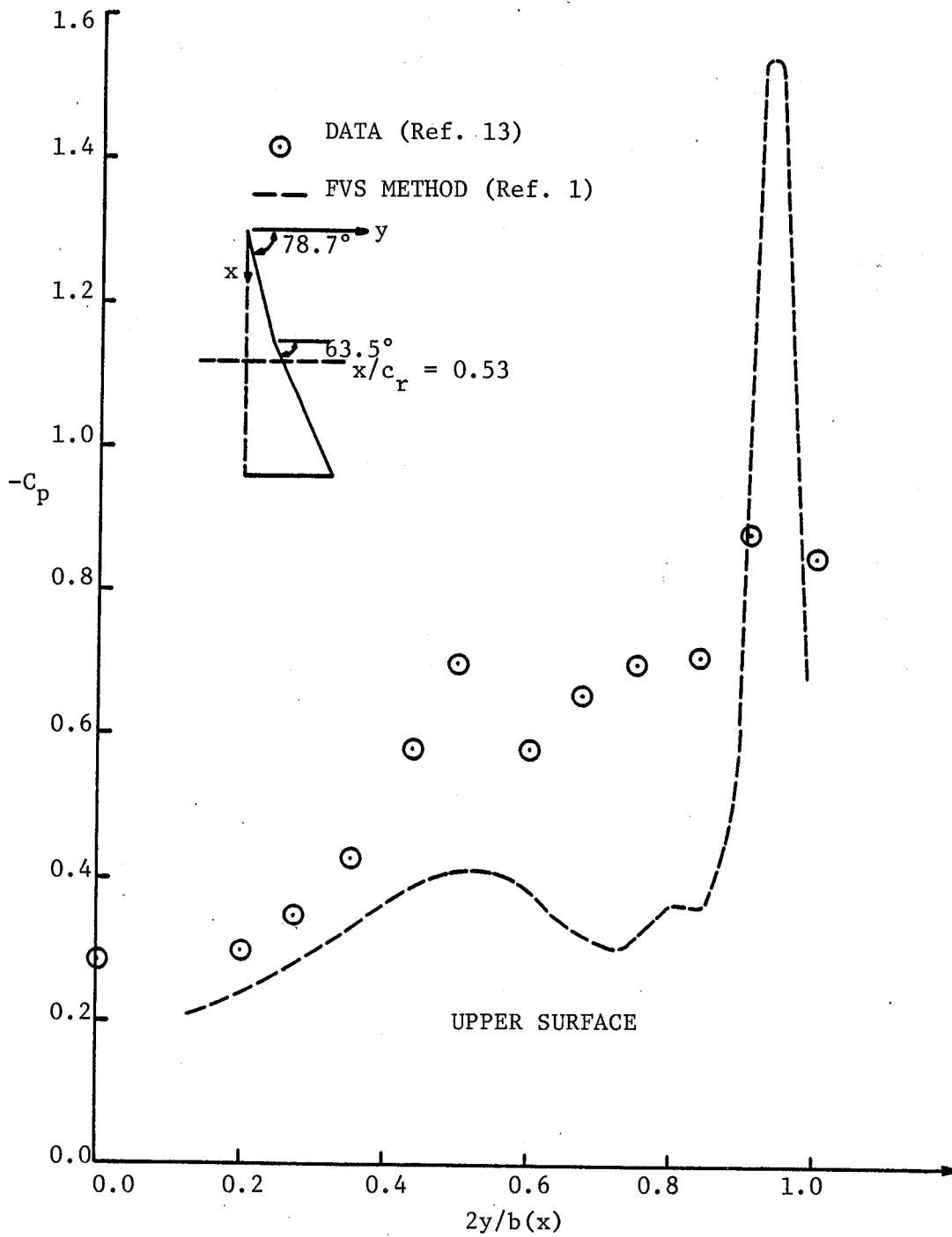


Figure 17. Spanwise pressure distributions for  $A = 1.83$  flat double delta wing at  $\frac{x}{c_r} = 0.53$ ,  $\alpha = 10^\circ$ , and  $M = 0.9$ .

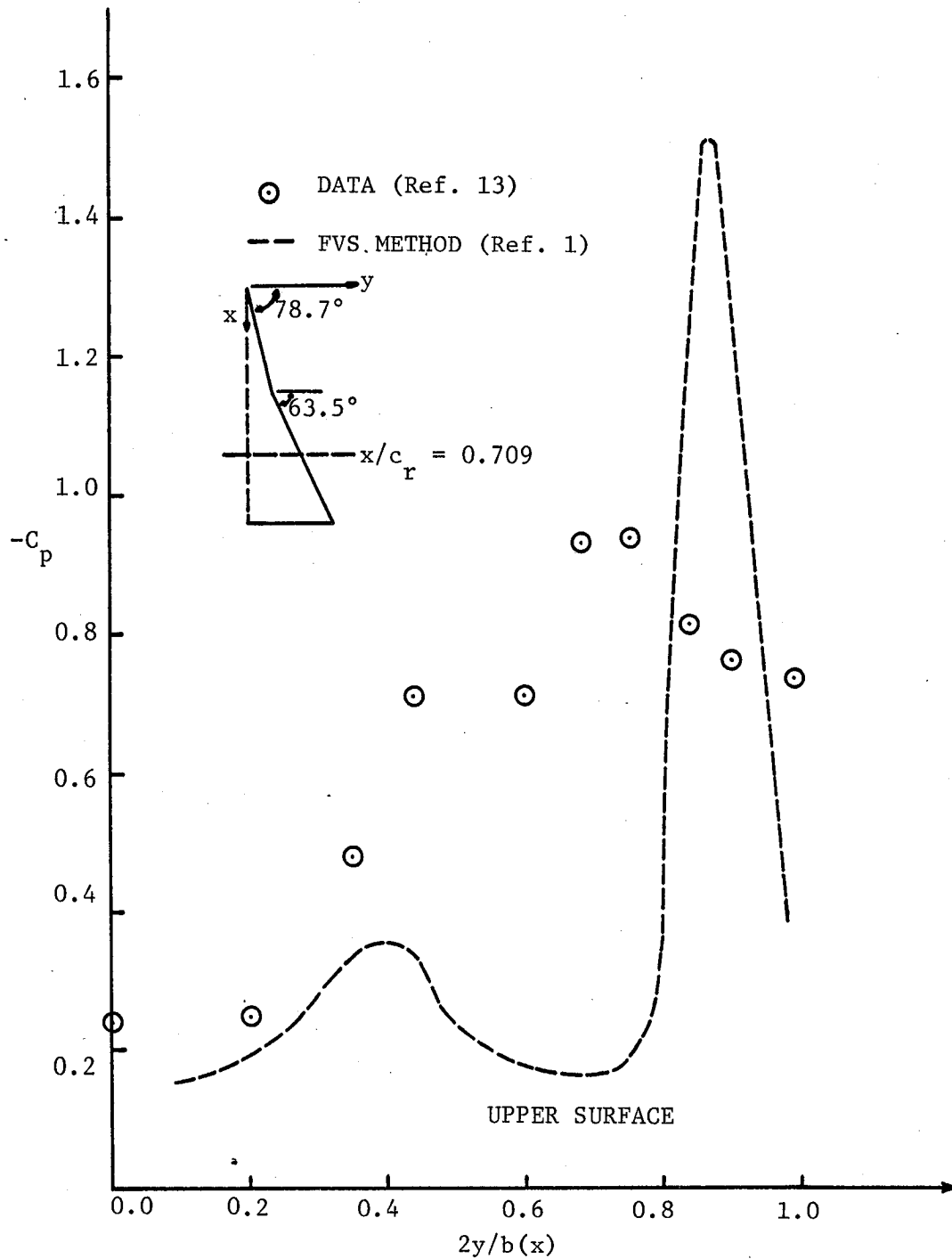


Figure 18. Spanwise pressure distributions for  $A = 1.83$  flat double delta wing at  $\frac{x}{c_r} = 0.71$ ,  $\alpha = 10^\circ$ , and  $M = 0.9$ .

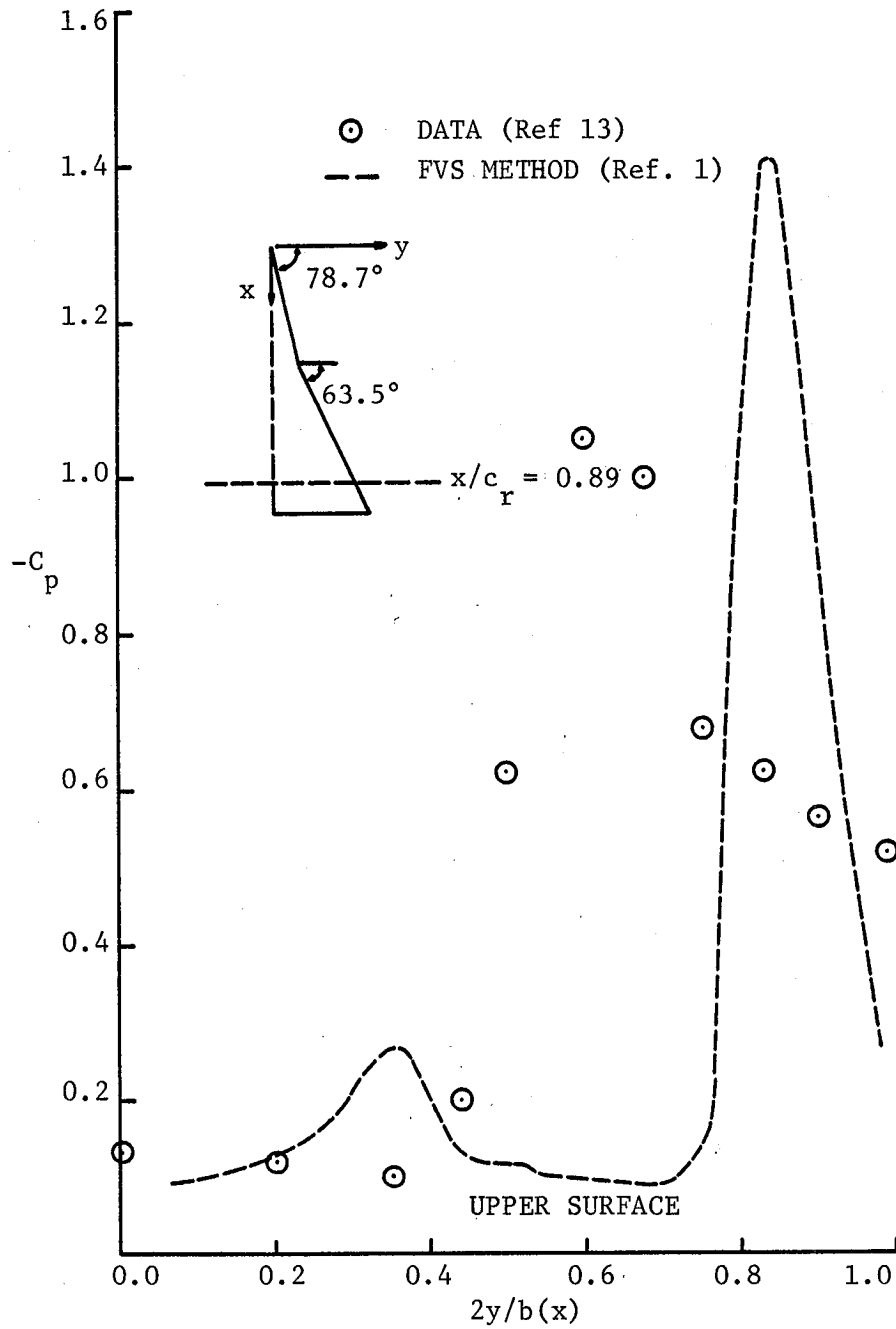


Figure 19. Spanwise pressure distributions for  $A = 1.83$  flat double delta wing at  $\frac{x}{c_r} = 0.89$ ,  $\alpha = 10^\circ$ , and  $M = 0.9$ .

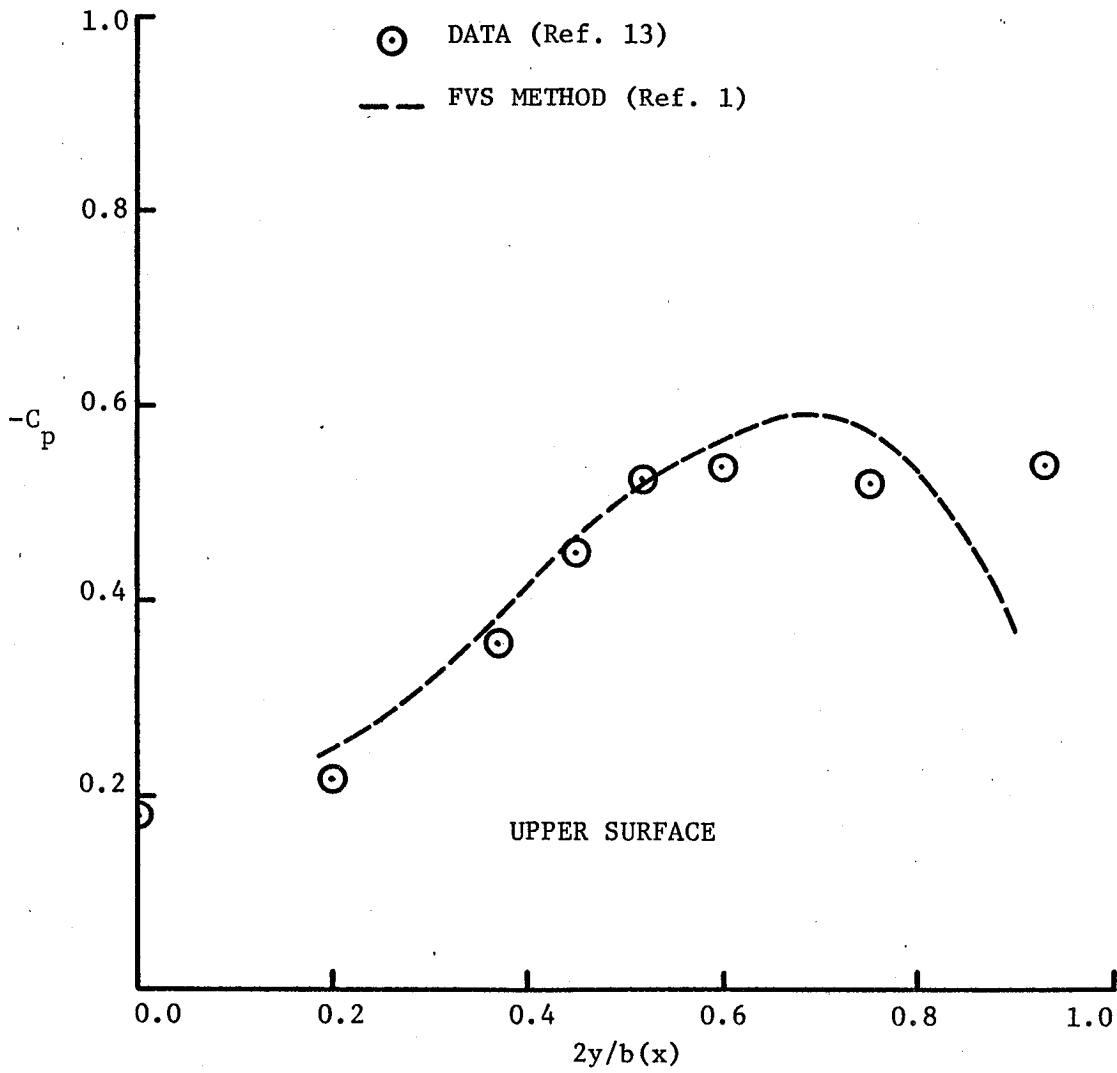
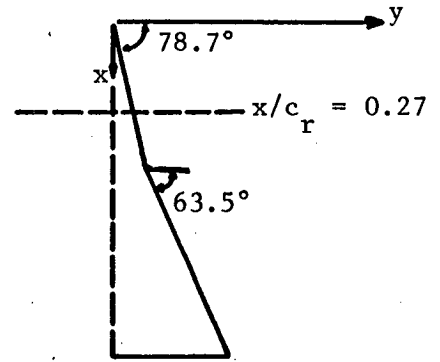


Figure 20. Spanwise pressure distributions for  $A = 1.83$  flat double delta wing at  $\frac{x}{c_r} = 0.27$ ,  $\alpha = 15^\circ$ , and  $M = 0.9$ .

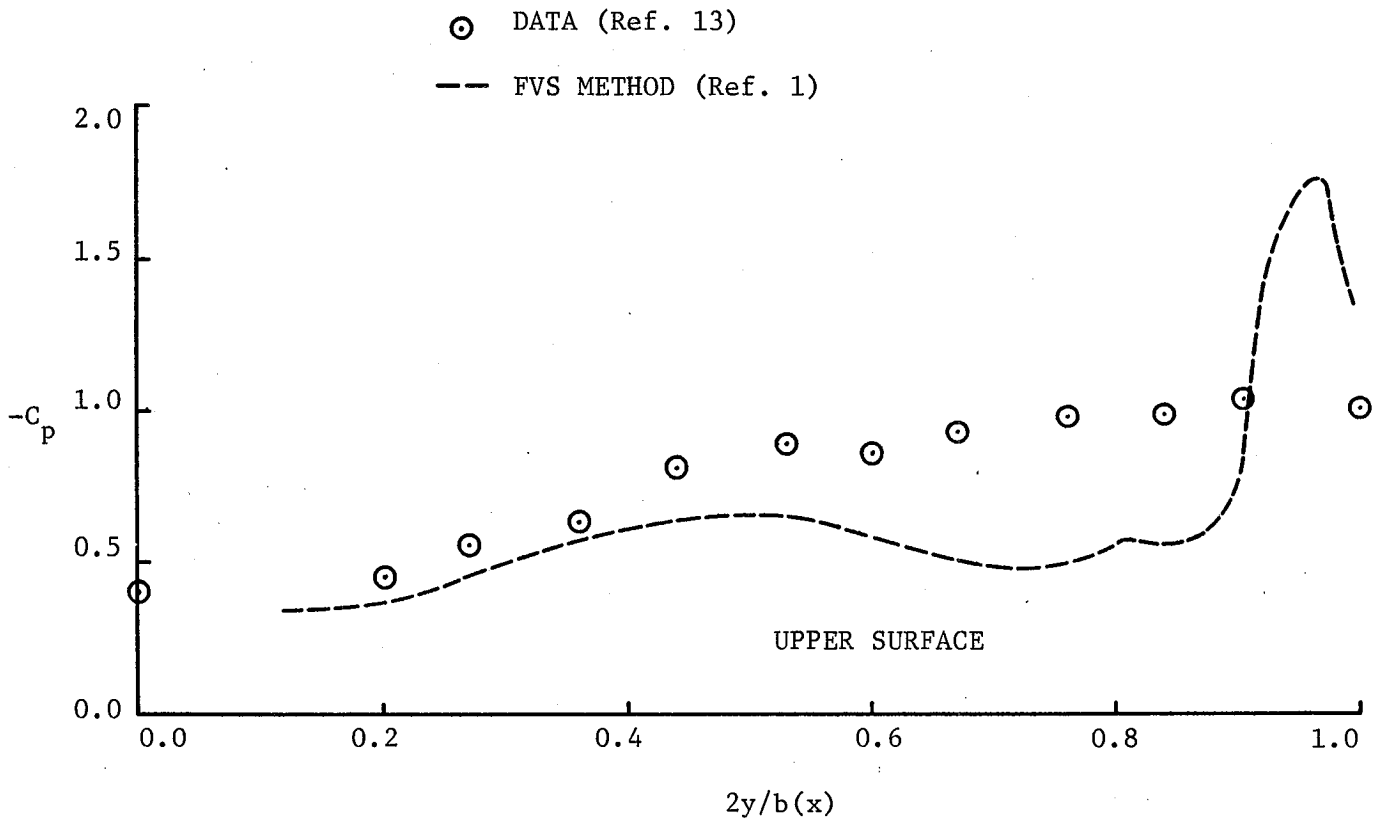
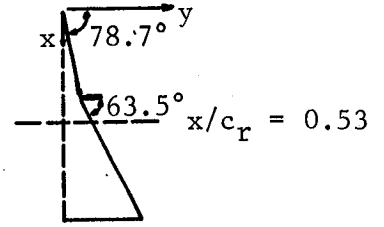
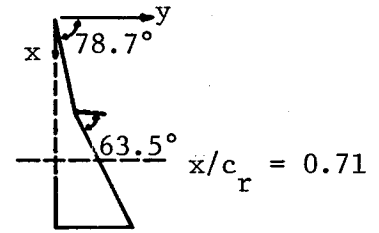


Figure 21. Spanwise pressure distributions for  $A = 1.83$  flat double delta wing at  $\frac{x}{c_r} = 0.53$ ,  $\alpha = 15^\circ$ , and  $M = 0.9$ .



○ DATA (Ref. 13)  
 --- FVS METHOD (Ref. 1)

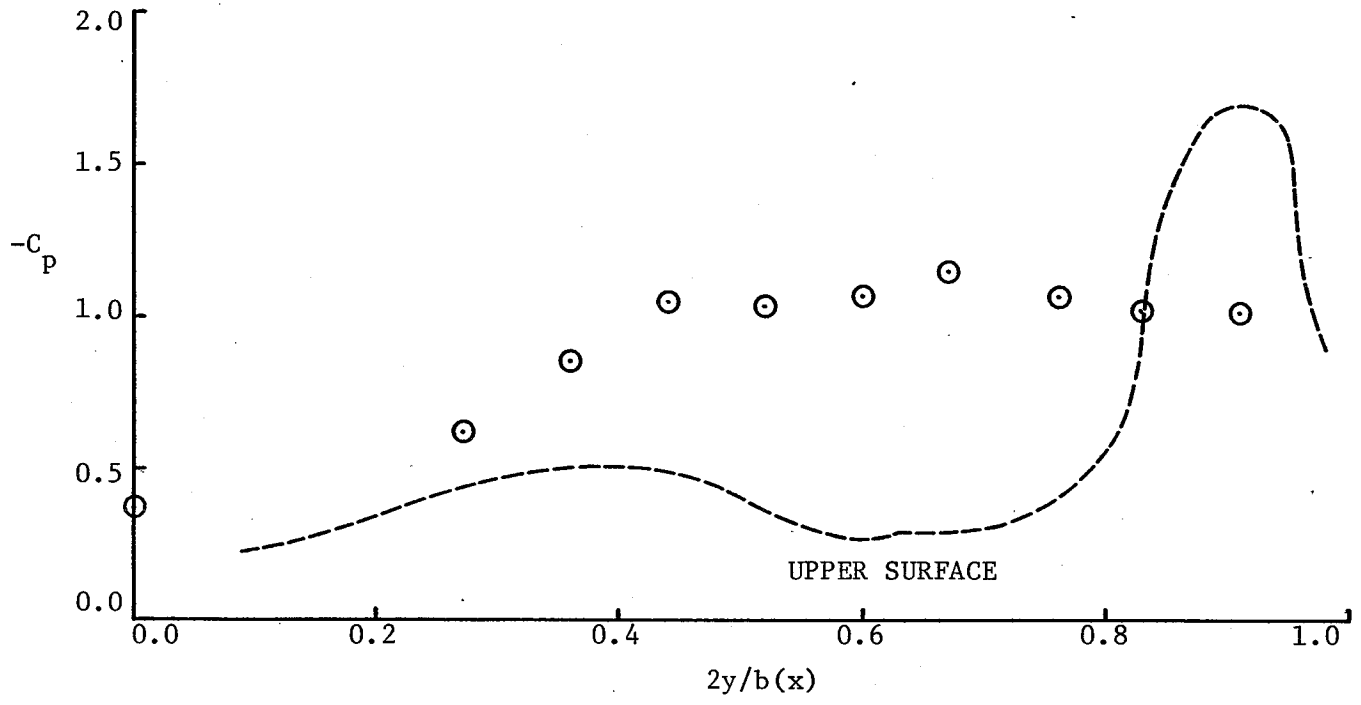
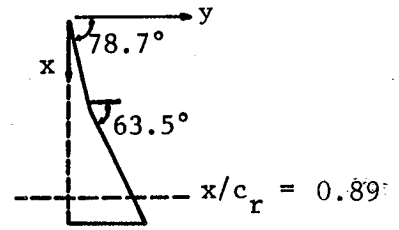


Figure 22. Spanwise pressure distributions for  $A = 1.83$  flat double delta wing at  $\frac{x}{c_r} = 0.71$ ,  $\alpha = 15^\circ$ , and  $M = 0.9$ .





○ DATA (Ref. 13)  
 --- FVS METHOD (Ref. 1)

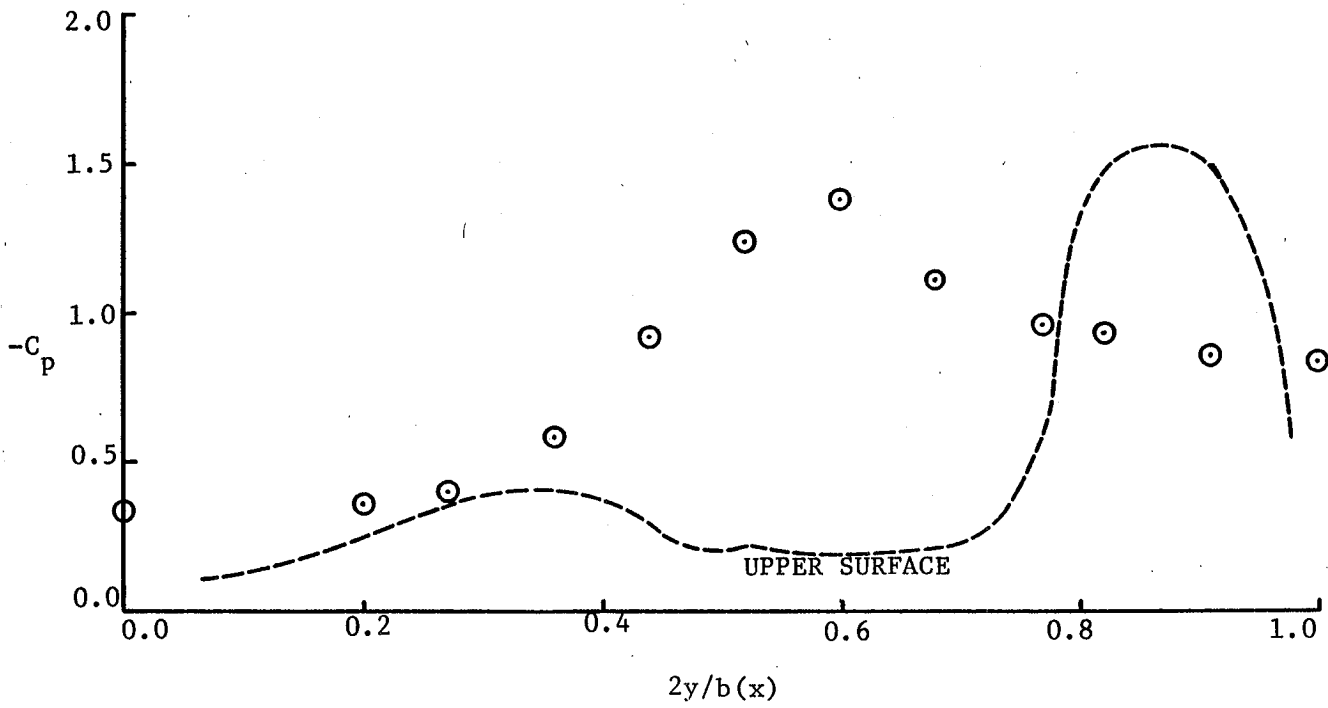


Figure 23. Spanwise pressure distributions for  $A = 1.83$  flat double delta wing at  $\frac{x}{c_r} = 0.89$ ,  $\alpha = 15^\circ$ , and  $M = 0.9$ .

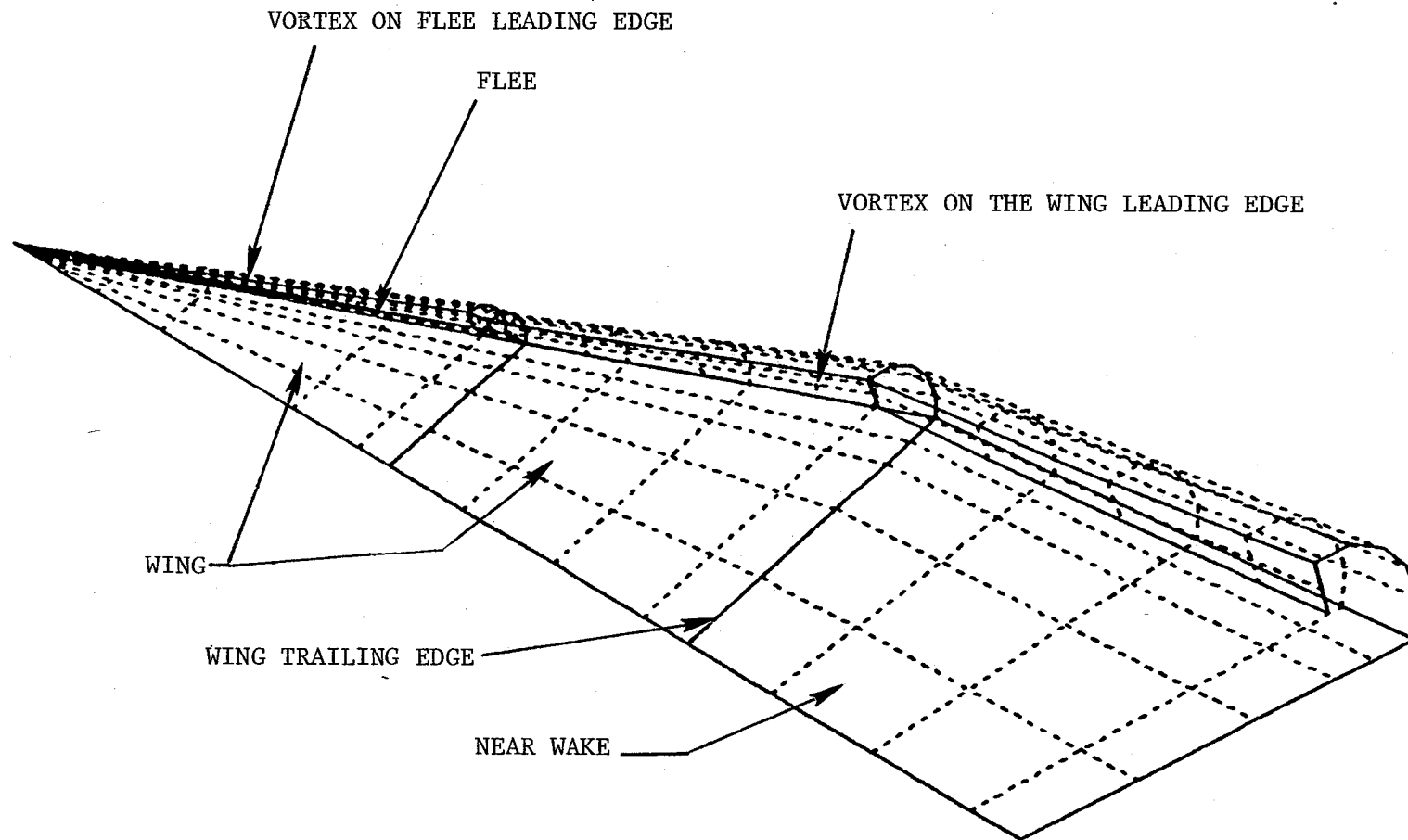


Figure 25. DM-1 glider, with vertical fin removed and FLEE attached, modeled by FVS method.

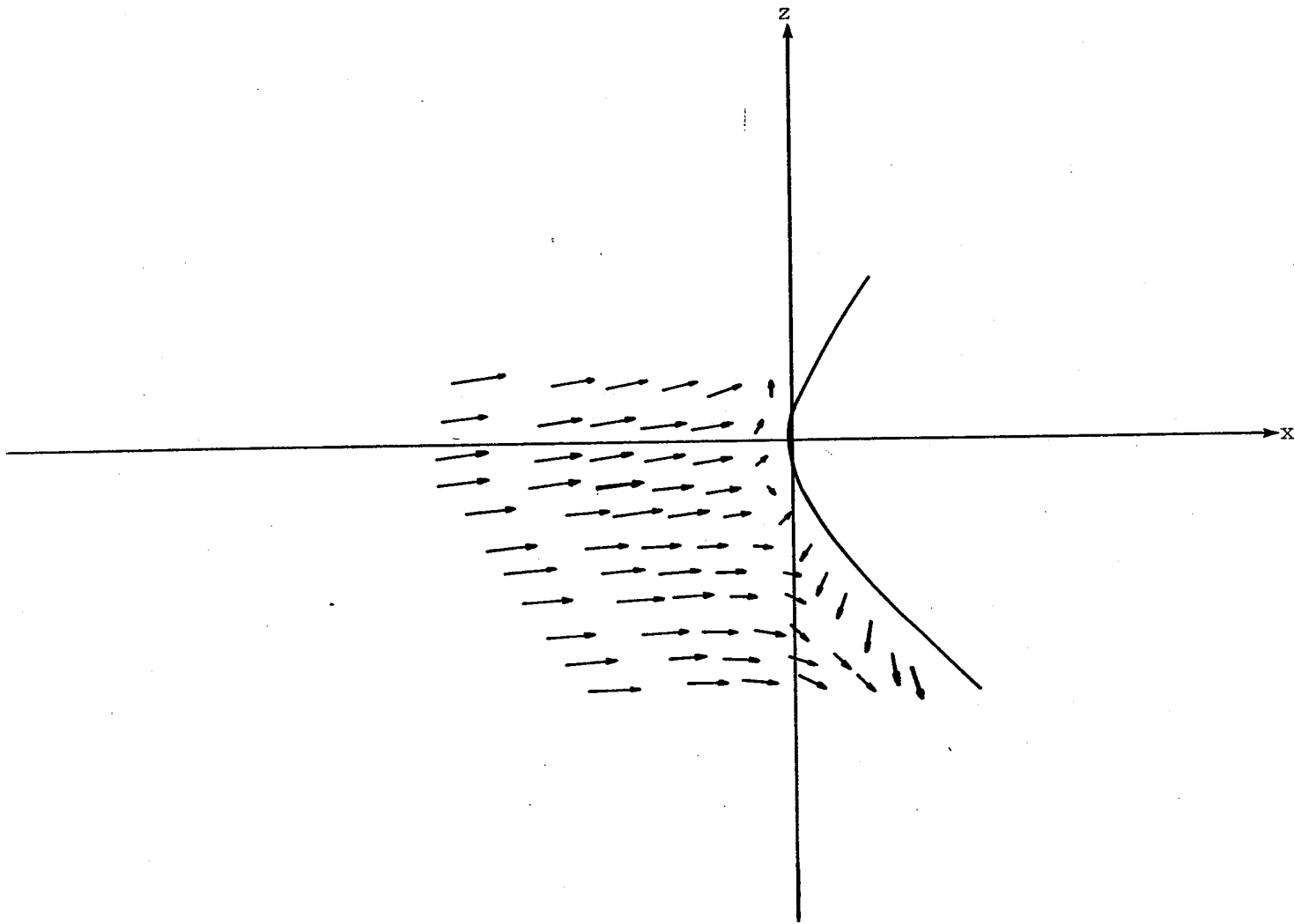


Figure 25. Velocity field for a thick delta wing at  $y = 0$ , and  $\alpha = 6.16^\circ$ .

NASA Technical Library



3 1176 01432 9057